Assessment of delay-and-sum algorithms for damage detection in aluminium and composite plates

To cite this article: Z Sharif-Khodaei and M H Aliabadi 2014 *Smart Mater. Struct.* **23** 075007

View the article online for updates and enhancements.

Assessment of delay-and-sum algorithms for damage detection in aluminium and composite plates

Z Sharif-Khodaei and M H Aliabadi

Department of Aeronautics, Imperial College London, South Kensington Campus, Roderic Hill Building, Exhibition Road, SW7 2AZ London, UK

E-mail: z.sharif-khodaei@imperial.ac.uk and m.h.aliabadi@imperial.ac.uk

Abstract

Piezoelectric sensors are increasingly being used in active structural health monitoring, due to their durability, light weight and low power consumption. In the present work damage detection and characterization methodologies based on Lamb waves have been evaluated for aircraft panels. The applicability of various proposed delay-and-sum algorithms on isotropic and composite stiffened panels have been investigated, both numerically and experimentally. A numerical model for ultrasonic wave propagation in composite laminates is proposed and compared to signals recorded from experiments. A modified delay-and-sum algorithm is then proposed for detecting impact damage in composite plates with and without a stiffener which is shown to capture and localize damage with only four transducers.

Keywords: damage detection, Lamb wave, structural health monitoring, composite stiffened panel, delay-and-sum algorithm

(Some figures may appear in colour only in the online journal)

1. Introduction

Structural health monitoring (SHM) techniques are increasingly being considered as a potential method to improve aircraft safety and reliability, possibly leading to lighter composite structures with the ability of detecting barely visible impact damage (BVID). The maintenance activity and operational cost can be reduced as a direct result of the SHM system. SHM techniques are based on a network of actuators and sensors, built into or mounted on the structure, which constantly monitor its status with minimal human intervention resulting in damage detection with the aim of shifting schedule-driven maintenance to condition based.

Piezoelectric (PZT) materials are one of the most attractive types of transducers, due to their small size and low power consumption, and their ability to be used both for actuation and monitoring of the structure. The direct and converse PZT effects make the PZTs attractive for both passive and active sensing. Passive sensing can be used for impact detection (Sharif-Khodaei *et al* 2012, Qiu *et al* 2013) and identification

(Ghajari *et al* 2013) and active sensing leads to damage detection and characterization (Su and Ye 2009). In addition, PZTs can be used for measuring the electro-mechanical impedance of the structure which can be used for self-diagnosis of the SHM system together with active sensing (Schwankl *et al* 2013). Ultrasonic guided wave (UGW) based techniques are amongst the most effective methods for active sensing in plate-like structures owing to their sensitivity to small defects, low attenuation and large scanning areas. Once UGWs are actuated, their propagation properties depend on the media through which they travel. The presence of damage or defects can alter their propagation and allow damage detection and characterization when a sensor network is used. The sensor number and layout can then be optimized (Mallardo *et al* 2012) to result in a system with high probability of detection (PoD).

There are various proposed UGW based techniques which are generally performed using a 'baseline' signal referring to the pristine state. The new measurements from the current state of the structure (possibly from a faulty state) are compared with the baseline signals and any significant change above a set

threshold indicates damage. The most straightforward method is to subtract the pristine signals from the signals acquired at the inspection time and to apply a triangulation technique based on time of flight of the damage reflected signal to locate the damage (Kessler *et al* 2002, Diamanti *et al* 2005). This approach is effective for simple and small structures. Nevertheless, for a complex structure such as stiffened panels, where stiffeners and frames cause additional reflections, the analysis of Lamb Waves becomes increasingly difficult.

Recently, attention has been focused on 'baseline free' techniques since obtaining a reliable baseline in practice is challenging due to environmental effects, manufacturing processes and operational conditions. The time-reversal method (TRM) has been proposed to mitigate the need for a baseline signal. This method involves time-reversing and re-transmitting the signals which have been captured by a sensor array. Wang *et al* (2004) have developed a synthetic time-reversal imaging method and reported the method to successfully detect a mass bonded to a plate, but it has not been tested for a damaged plate. Sohn *et al* (2007) applied TRM to detect delamination in composite plate. However, for a plate of size 60.96×60.96 cm 16 transducers were used, which adds up to 240 different actuator-sensor pairs which is very time consuming and computationally expensive. Watkins and Jha (2012) presented a modified TRM which reduced the hardware requirements significantly and successfully detected the presence and severity of impact damage in a composite plate. However, the TRM on its own is not capable of locating the damage. One approach is to combine the TRM with elastic nonlinearity to localize damage with a proper imaging technique. To obtain the response of the structure a laser vibrometer or numerical simulation can be used as presented by Scalerandi *et al* (2008). The nonlinear TRM method can be very effective for simple and small structures where receiving the signals at various locations is not time consuming or computationally expensive. However, the proposed method will not be effective for recording the response of large complex structure such as stiffened panels as a large area needs to be scanned.

Radzieński *et al* (2013) have applied changes in propagating waves for damage detection in a stiffened aluminium plate. Laser vibrometers were used as sensors to record full wavefield measurements at many points. Non-contact measurement with laser vibrometry gives information of very high resolution on the propagating waves. Moreover, non-contact measurements avoid reflections from embedded sensors which could make the signal processing more difficult in structures with complex geometry. Damage is then detected by the application of the root mean square and the energy distribution analysis. The methodology was tested on an aluminium stiffened panel where damage was introduced in the form of removing some rivets as well as an additional mass attached to the plate surface which does not validate the method for the detection of impact damage in composites. The proposed method cannot be treated as online because processing a large amount of data and collecting the measurements takes too long.

Most of the proposed Lamb wave based damage detection techniques involve baseline comparisons of signals. Once the presence of damage is known in the structure, to locate and characterize the damage a network of transducers are required. The sensor signals in their discrete form carry too much information to be used directly for damage characterization. Consequently, various identification algorithms are developed based on a variety of feature extraction techniques. A comprehensive selection of methodologies are reported in Su and Ye (2009). Different signal features can be used to define a damage index for localizing and characterizing damage. Ostachowicz *et al* (2009) have proposed a damage localization algorithm based on phased array transducers distributed in a ring pattern. This method has shown to be effective for damage localization, by transforming the signals from their time domain to their spatial domain, nonetheless a large number of sensors in close vicinity of the damage was necessary (12 sensors in a circular area of 80 mm diameter) which makes it an attractive method for localized searches in structural hot-spots. The same group (Kudela *et al* 2008) have also tested a second algorithm based on constructing a damage influence map of the structure based on comparison of the baseline and current signals at defined time windows (in a similar manner to delay-and-sum algorithm). They used spectral elements to model the wave propagation in a multi-layer composite and successfully detect cracks in the structure. Ben *et al* (2012) have identified changes in dispersion characteristics and attenuation of Lamb waves with respect to its undamaged state to identify damage. In addition, the detected damage was introduced as (1) a cut partway through the bar and (2) a circular hole. Thus the applicability of the method when damage is introduced as fibre/matrix breakage or delamination remains uncertain. Furthermore, the presence of openings, stiffeners and frames will alter the wave propagation properties. Therefore, the developed algorithms remain to be tested on more complex structures to assess their general applicability.

Zhao *et al* (2007) have developed an algorithm called reconstruction algorithm for probabilistic inspection of defects (RAPID) which adds the contributions of the signal differences, between the pristine and damage states, for all transducer pairs. They have successfully detected cracks and corrosion in a metallic skin panel of a wing box. However, the method remains to be tested for composite structures with impact damage.

Fromme *et al* (2006) have effectively located defects in a steel plate with stiffener applying a delay-and-sum imaging method where received signals are delayed and summed according to an appropriate spatial rule for each point on the image. Michaels (2008) has utilized a damage detection method based on a delay-and-sum imaging algorithm to accurately determine a notch and corrosion on an aluminium plate. In addition, the effect of the temperature on the baseline signals was investigated. However the algorithm was tested only for isotropic plates where the group velocity is uniform in all directions. Qiu *et al* (2013) have proposed a damage detection algorithm for large scale composites where first the damage area is identified by a damage index merging algorithm. Afterwards, a delay-and-sum algorithm is performed only in the identified subarea. They have showed successful

detection of multiple damages in a composite wing panel. Nevertheless, artificial damages were introduced by adding solid adhesive tapes. The validity of the method for detection of inter-laminar delamination, which is common type of impact damage in composite materials, remains to be tested.

Imaging algorithms together with damage indices have shown to be successful in damage detection and localization. In particular, the delay-and-sum method has reported to be effective for impact damage detection in composite structures. Different signal features can be used for introducing a damage index, which plays an important role in the effectiveness of the algorithm. Most of the reported methodologies based on the delay-and-sum technique have been developed and tested for isotropic materials or composite plates of simple geometries with constant thickness and/or no discontinuities and a large number of transducers. The types of damage investigated are mainly through holes or added mass which are not representative of BVID. Therefore the applicability of the techniques on real structures with the corresponding types of damage still remains questionable.

In addition, to be able to implement an SHM system as a non-destructive inspection (NDI) technique for an actual structure, issues such as environmental effects, durability of the system, PoD, probability of false alarm (PoFA) and reliability of the system must be investigated. Different PoD approaches have been proposed and investigated by (Kessler *et al* 2011, Cobb *et al* 2009 Lindgren *et al* 2011). In order to fulfil the required reliability regarding conventional NDI procedures, the guideline (JSSG 2006) obliges the NDI technique to demonstrate '90 per cent probability and a 95 per cent confidence level'. For any developed SHM system, an appropriate procedure to assess the PoD of the system must be considered (Soejima *et al* 2012). This will involve detection of different defect size, type and location which indicates a huge number of panels to be damaged and tested. This might not be realistic as it can be very expensive and time consuming to test on physical structures. Therefore we propose a valid FE model to replace the huge number of tests necessary for evaluating the proposed SHM system.

This paper is divided into two parts: the first part describes the FE model for sensing and actuating of Lamb waves in aluminium and composite plates, validated with experimental results (sections 2 and 3). The second part assesses various delay-and-sum algorithms for damage detection in composite panels. The delay-and-sum algorithms proposed by Michaels (2008) and Zhao *et al* (2007) are evaluated for detecting impact damage in composite panels (section 4) and an improved algorithm is proposed and tested (section 5). The last section (section 6) summarizes and concludes the results of the proposed damage detection method.

2. Experimental set up

In order to develop a valid numerical model for wave propagation in isotropic and anisotropic composite plates, the numerical results must be validated against experimental
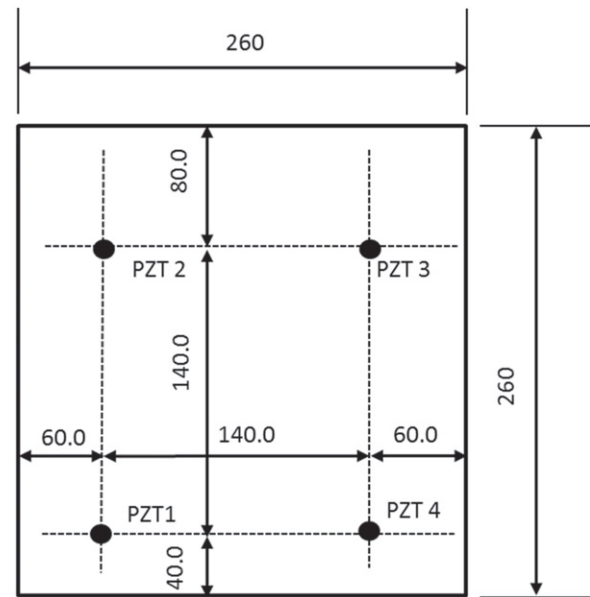

Figure 1. Schematic of the aluminium panel.

signals. In this section both aluminium and composite panels have been tested at different actuation frequencies for pristine and damaged cases. The aluminium plate was damaged by drilling a hole in the plate and the composite panels were impacted to create damage. In section 3 the experimental results are used for validating the proposed numerical model which can later be utilized in damage detection techniques and to compute the PoD of the designed SHM system.

2.1. Aluminium plate

Four PZT transducers were attached with epoxy to an aluminium plate $260 \times 260 \times 13$ mm as shown in figure 1. The material properties of the plate are Young's modulus $E = 72.7$ GPa, Poisson's ratio $\nu = 0.33$ and density $\rho = 2700$ kg m^{-3}. The transducers used were type PIC255 with properties of $E = 70.5$ GPa, $\nu = 0.31$, density $\rho = 7800$ kg m^{-3}, dielectric constant $K_3 = 1685$, PZT charge coefficient $d_{31} = -130 \times 10^{-12}$ m v^{-1} and thickness of 0.5 mm. The transducers are bonded to the plate using superglue.

Signal generation and data acquisition was performed with an NI data logger. The signal generator is an NI PXIe-5450 with a sample rate of 400 MS s^{-1}. The maximum voltage that the generator can output is ± 1 V, therefore an A-303 high voltage amplifier was used to amplify the signal. The influence of different parameters such as boundary conditions, environmental effects, connections, etc on the acquired signal was studied and reported in details by Salmanpour (2013). The data acquisition is carried out by NI PXI-5105 high frequency digitizer with eight simultaneous channels. The sampling frequency for the data acquisition card is 60 MS s^{-1}. The plate was actuated at different frequencies and the pristine signals were recorded in all sensors. This was repeated for all the transducers acting once as actuator.
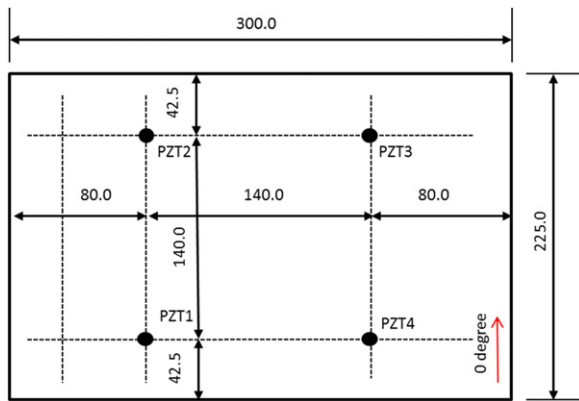
Figure 2. Geometry of the composite panel.

2.2. Composite plate

A carbon-fibre epoxy composite plate was manufactured with eight unidirectional plies made from M21/T700 with a layup of $(45/−45/0/90)_s$. The thickness of each ply is 0.262 mm which results in overall thickness of 2.096 mm. The zero degree fibre orientation is shown in figure 2. The circular transducers used are type NEC51 having 10 mm diameter and 1 mm thickness. The material properties of the pre-peg and the sensors are summarized in section 9.1 and 9.2.

The plate was actuated at different frequencies ranging from 50 to 500 kHz in order to find the most effective frequency to be used as a baseline for damage detection. The best excitation frequency (the least attenuation) was around 250 kHz which resulted in the highest amplitude of the sensor signal. An amplifier had to be used for higher excitations as the output was too low. It was noticed that the amplifier introduced a noticeable lag in the actuation signal shown in figure 3(a). The sensor signals were then shifted by this time lag to calculate the correct time of arrival (ToA).

The raw acquired signals are very noisy and appropriate filters must be applied before they can be used in any damage detection algorithm. To check the repeatability of the experiment and to enhance the signal-to-noise ratio, each sensor data was recorded 15 times and averaged. To remove the noise a low pass Butterworth filter of 4th order has been used. An example of the signal before and after de-noising is shown figure 4. The signal pre-processing is studied in more detail in section 5.1.

Moreover, the signal generation and the acquisition channels are next to each other in the data logger, and the interaction of both circuits causes an undesired effect on the signals transmitted in the data acquisition channel, known as cross-talk, see figure 4.

Damage detection using Lamb waves is highly dependent on the velocity of the propagating wave. The group velocity is calculated by calibrating the arrival times of the direct waves travelling between actuator and sensor. Therefore, to ensure a reliable measure of the group velocity, it is of high importance to remove the cross-talk interfering with the detection of the ToA of the signals. For each transducer path the arrival time of the first wave packet was measured and then calibrated with the transducer separation distance as plotted in

figure 3(b). The best fit is a linear regression where the slope gives the group velocity of the first arrival mode (S_0) and the intersection with time axis is a fixed time offset t_{off}. Measuring the ToA for each path is addressed in more detail in section 5.2 as part of the detection algorithm (figure 5).

After the pristine signals were recorded the plate was impacted to induce damage. The impactor was a hemisphere 20 mm in diameter and resulting in impact energy of 5.83 J (2.2 m s^{-1} velocity, 2.41 kg mass). The impact was carried out using a drop tower INSTRON CEAST 9350 machine (figure 6). The impact energy was chosen in order to cause an impact force which is 10% above the delamination threshold force calculated according to equation (9) defined in Ghajari *et al* (2013). The contact force was measured from a finite element impact analysis.

After the plate was impacted and damaged, it was actuated with the same frequency range as for the pristine state and sensor signals were recorded.

To observe the influence of more complex geometries a composite plate, identical to the one presented in figure 2, was constructed with additional stiffener 190 mm × 15 mm bonded in the middle of the plate, see figure 7(a). The sensor signals for the plate with and without a stiffener are compared to see the influence of the stiffener on the wave propagation. It can be seen in figure 7(b) that the sensor signals attenuate and reflect when passing through the stiffener. The amplitude of the first mode is significantly smaller (∼60%) than the plate without a stiffener. The reason for this is that when the propagating wave reaches the stiffener it decomposes into two components: one transmitting through the skin underneath the stiffener and the other component propagating along the stiffener. The stiffened plate was impacted under the stiffener at the middle of the plate to cause damage. Sensor signals before and after the impact were recorded for damage detection.

3. Numerical modelling technique

Wave propagation in plates can be modelled by solving the equation of motion either analytically (Rose and Nagy 2000), semi-analytically (Bartoli *et al* 2006) or by means of numerical methods. Analytical studies are complex, have limited application and they become computationally expensive when applied to real engineering structures due to their size and complexity. The numerical approaches include the finite difference method, finite element method (FEM) (Koduru and Rose 2013), boundary element method (BEM) (Fedelinski *et al* 1997), combined FEM/BEM approach (Zou *et al* 2014), mesh-less method (Wen and Aliabadi 2008), spectral element method (Kudela *et al* 2007, Peng and Meng *et al* 2009), mass spring lattice method (Delsanto and Scalerandi 1998, Yim and Sohn 2000). However effective the proposed models are, the most cost-effective approach, for modelling real aircraft structures of complex geometry and lay-up, is FEM-based simulation with commercially available software such as ABAQUS, ANSYS, PATRAN. Moreover, the PZT transducers can be modelled analytically (Ma
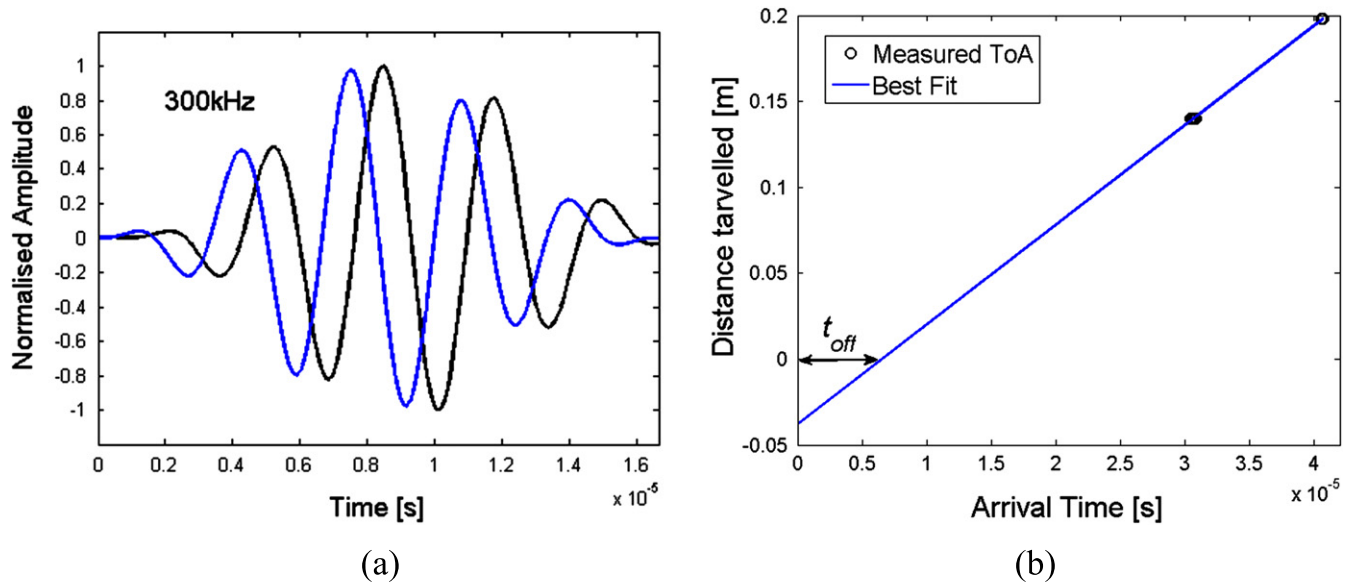
(a)   (b)

Figure 3. (a) Delay in actuation signal due to amplification, (b) measured velocity as function of ToA and travelled distance.
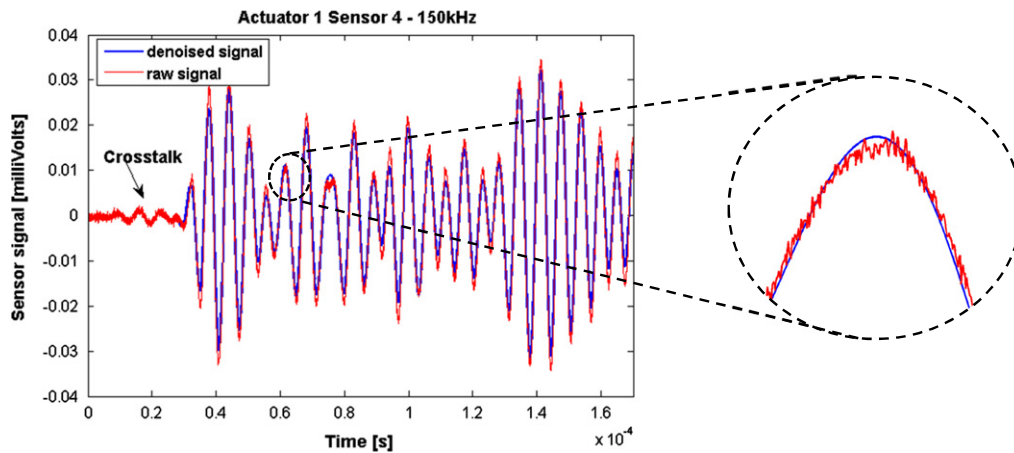

Figure 4. Sensor signal before and after filtering.

et al 2012), semi analytically (Benedetti *et al* 2010) or using numerical methods (Mo *et al* 2012).

A concise overview of the FEM and simulation of wave propagation in plates can be found in Su and Ye (2009) and Lee and Staszewski (2003). Some aspects of FE modelling of wave propagation using explicit dynamic analysis are reported by Yang *et al* (2006). Yang *et al* have modelled isotropic and quasi-isotropic composite laminates using 3D solid and 3D shell elements. Nevertheless, only the group velocity of the waves was validated against the experimental data and not the waveform. To the authors' knowledge, few researchers have validated FE modelling of wave propagation in composite laminates against experimental signals (waveform and velocity). Therefore a detailed study is carried out in the next section for both an isotropic (aluminium) and a composite laminate plate.

3.1. Aluminium plate

The first case study is the aluminium plate with four surface-mounted PZT transducers described in section 2.1. The

analysis has been carried out using the commercial program ABAQUS. An Explicit dynamic step was created for the analysis and to allow sensing and actuating.

Wave propagation is a dynamic problem and the validity of the results depends very much on the correct mesh size and stable time increment. In a study carried out by Salmanpour (2013) at Imperial College, the mesh convergence was evaluated for the Al panel with different numbers of nodes per wavelength (NPW), stable time increments and excitation frequencies. It was shown that at the recommended minimum NPW of ten (Alleyne and Cawley 1991), the waveform of the sensor signal did not resemble a tone-burst five-cycle sinusoidal signal which was the actuation signal. The first and second modes were well captured at 30 NPW; however some of the higher modes had some cut-off peaks. It was reported that 40 NPW, for conventional shell elements, was the converged value for sensor signals in the plate. Therefore for every model it is important to carry out a convergence study to be able to capture the correct waveforms of different
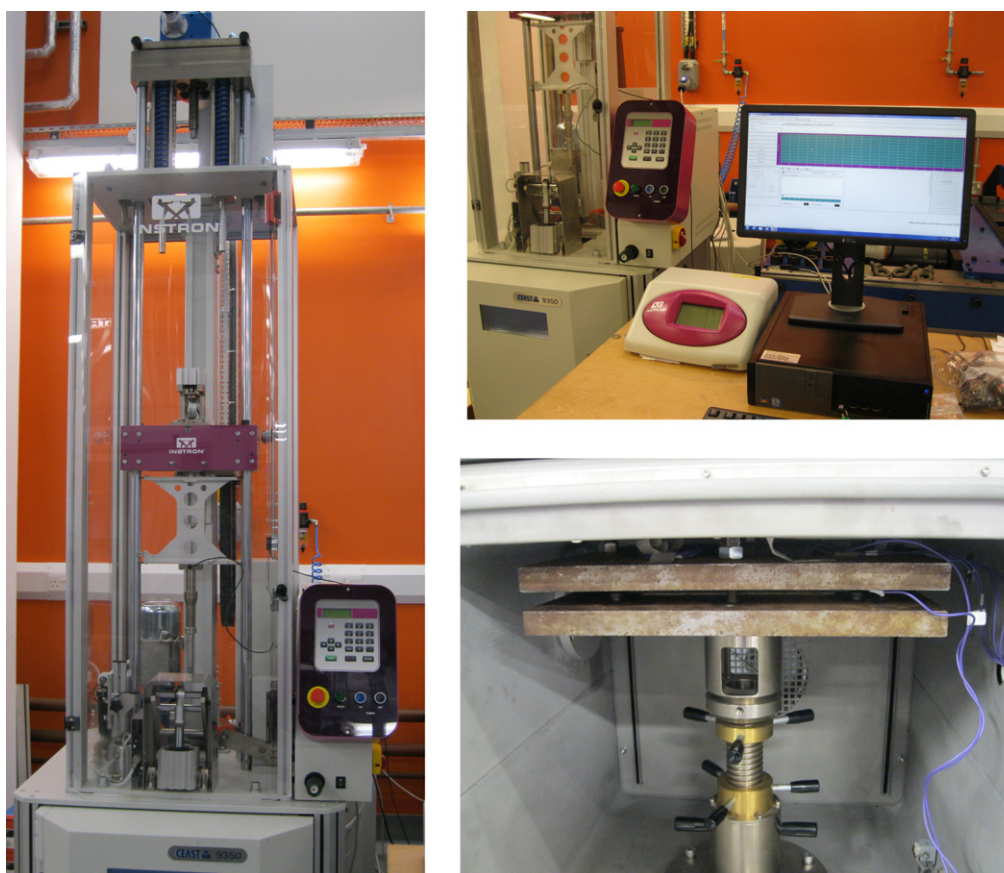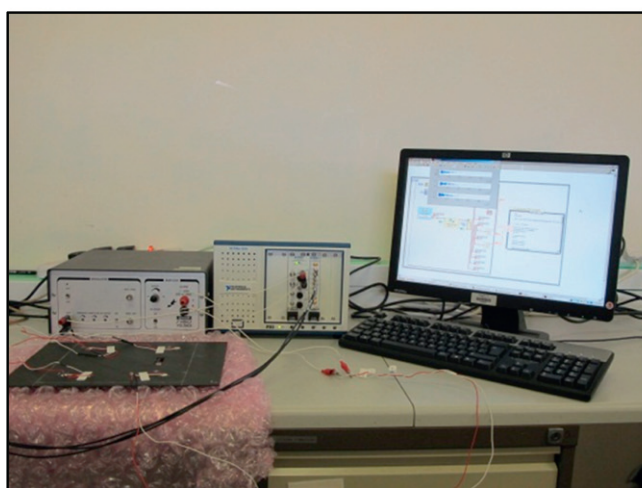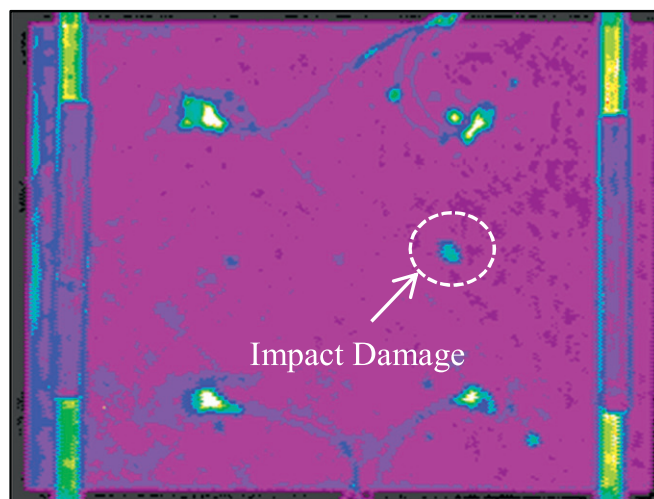
Figure 5. INSTRON CEAST 9350 machine used for impact test.


(a)

Impact Damage

(b)

Figure 6. Damage detection in composite plate—experimental results. (a) Experimental set-up. (b) C-scan image of impacted plate.

modes. For the Al plate in this work the mesh size and time increment corresponding to 40 NPW has been used.

The FE model was analysed with different element types to find the best modelling technique for wave propagation in a thin isotropic plate. The plate was modelled using shell (both conventional and continuum) and solid elements. Due to the nature of the analysis (dynamic) and the small mesh size requirements, solid elements (3D brick) will increase the computational cost substantially. There were no significant changes noticed when comparing results of the shell model with the 3D brick model for the homogenous plate (Salmanpour 2013). Therefore it is computationally more convenient to use a 2D shell model. There are two possible shell models in ABAQUS: conventional and continuum shell
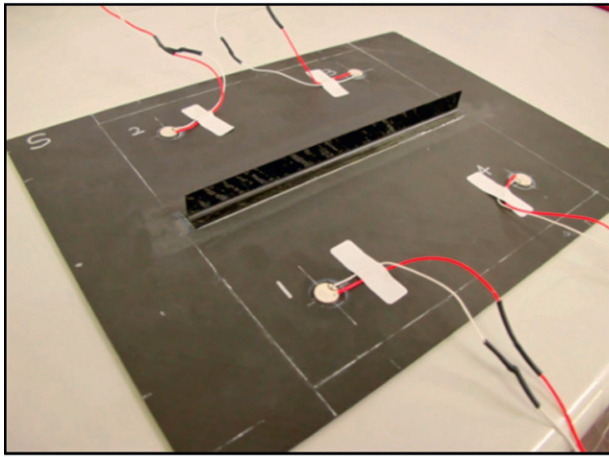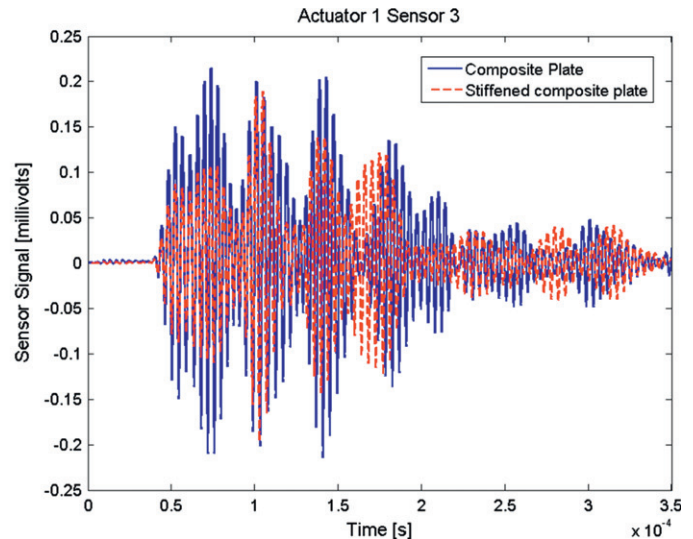
(a)   (b)

Figure 7. Composite panel with bonded stiffener. (a) Stiffened plate geometry. (b) Signals from stiffened and unstiffened plate.

models. Using conventional shell, the geometry is defined by a reference 2D surface and the thickness is defined through section properties. The elements have both displacement and rotation degrees of freedom. In contrast, continuum shell elements discretize the full 3D body and they only have displacement degree of freedom. The effect of both shell models on the wave propagation in the plate have been investigated and compared to the results published by Su and Ye (2009). The same geometry and layup has been used for this case study. First, the plate was modelled using conventional shell elements and it was realized that the choice of the reference surface of the plate (defined at mid-surface or top/bottom surface) has an important effect on the validity of the results. As depicted in figure 8, some of the modes can be missed entirely by choosing a different reference surface. By comparing the waveform with published results (Su and Ye 2009), it was concluded that the mid surface should be used as the reference surface. The discrepancy in figure 8(b) with published results is due to the boundary reflections as it was not specified what boundary conditions were used. However, the first A_0 and S_0 modes coincide well. After investigating the application of conventional shell elements, the aluminium plate shown in figure 1 was analysed. The PZT transducers were modelled using 3D brick elements. In Implicit analysis there is the option of using PZT elements. That means that the voltage can be directly applied to the terminals of the transducers and the corresponding strain response in the sensors are acquired through the electro-mechanical coupling of the elements. This is not an option in Explicit analysis using ABAQUS. Therefore the coupling between electrical and mechanical degrees of freedom is done through analytical relations between the voltage and radial displacement. SMART elements have been developed and applied which are capable of both sensing and actuating based on the electro-mechanical constitutive equation of a PZT wafer (Su and Ye 2009). To ensure the validity of the results

both Implicit and Explicit analysis were performed and the results were compared. As can be seen in figure 9(a), there is a very good agreement with both models (conventional and continuum shell elements).

Figure 9(b) shows the comparison of the experimental results against the FE analysis using conventional shell elements. The ToA of both waves match well, and the wave shapes agree in both cases, however there is a slight delay in the experimental signal which can be caused due to the experimental set up (amplifier, wiring, etc) or the damping effects in the plate which are absent in the numerical model. In general the signals matched well for 75 kHz excitation and the focus was then turned to composite panels which are more complex from the modelling perspective.

3.2. Composite panel

Many researchers have reported on numerical modelling and validation of homogeneous and isotropic plates. However, there are not many available reports on validating FE numerical models of wave propagation in anisotropic composite plates against experiments. Therefore, the focus of this section is on different modelling techniques for wave propagation in composite plates. The plate under consideration (section 2.2) has been modelled using shell elements (both continuum and conventional) and 3D brick elements. As depicted in figure 10(b), the first symmetric (S_0) and antisymmetric (A_0) modes in all three numerical models coincide. However, discrepancies start showing later on in the signal. This could be related to the shorter wavelength of higher modes (A_1, S_1,...) requiring a higher number of NPW, superposition of different modes and reflections from the boundary which are not identical in the different models. To support this idea, the displacement fields in the plate have been considered for all three models.
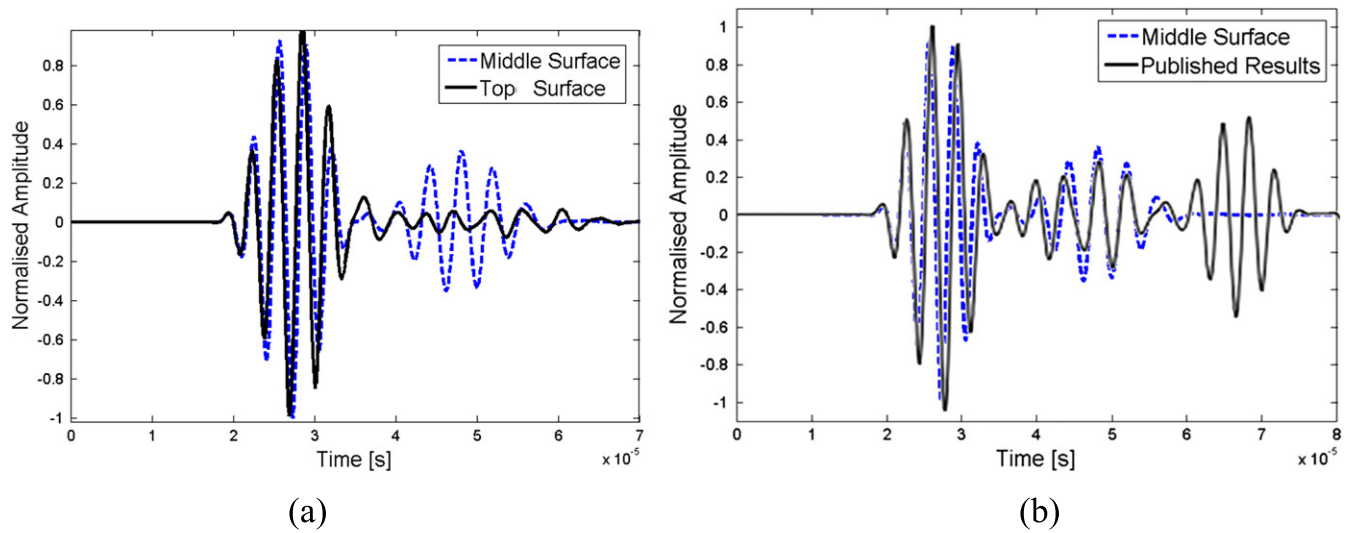
(a)   (b)

Figure 8. Influence of shell reference surface, comparison with published results by (Su and Ye 2009).

(a)   (b)
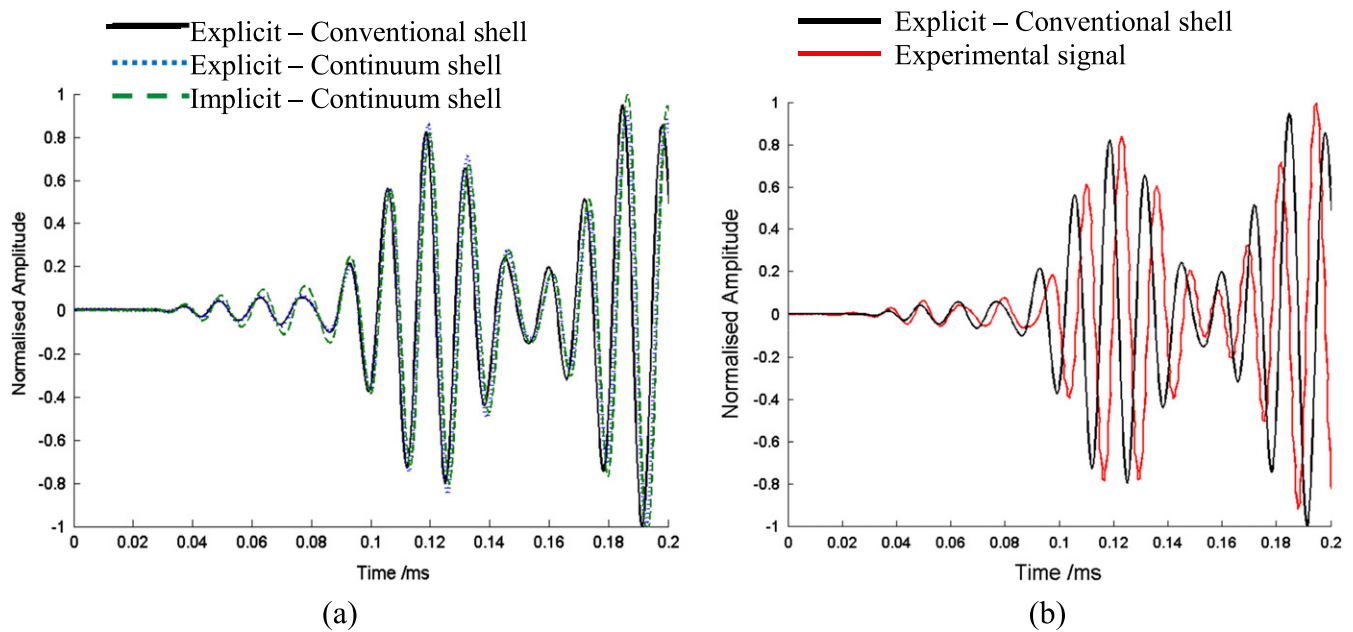
Figure 9. (a) Sensor signal for 75 kHz excitation frequency, experimental results versus different numerical models, (b) numerical model versus experimental results (path actuator 4—sensor 1).

Examining the propagation of the wave in the plate (figure 11), one reason why the solid element model differs from the shell models could be due to the dissimilar patterns in boundary reflected waves and superposition of different wave forms. The free boundary of the plate modelled with solid elements is a 2D surface, whereas shell elements are defined at the reference surface of the plate resulting in 1D boundary edge. The wave reflections from a surface and an edge can alter the propagation field in the shell and brick models. The discrepancies in the shell models can also be related to the difference in their degrees of freedom.

The results emphasize the need for a deeper investigation into various aspects of numerical modelling for wave propagation in composite laminates. For the proposed damage detection methodology in this work, the first wave modes are

used and since the first modes match quite well for all three models (figure 10(b)), there were no further investigations into the numerical analysis. Moreover, the numerical model has been adopted only for development purposes and the algorithm has been tested with sensor signals recorded experimentally, therefore the deeper investigation of numerical models is expected in future works. The proposed numerical model for acquiring sensor signals is based on conventional shell elements due to their computational advantages. The first mode Lamb wave from the conventional shell model is validated against experimental results (for both ToA and wave form of the first arrival mode), in figure 12 where the results for actuator 1–sensor 4 path is plotted.

The experimental signals are shifted by a fixed time delay which is caused by the amplifier and experimental setup as
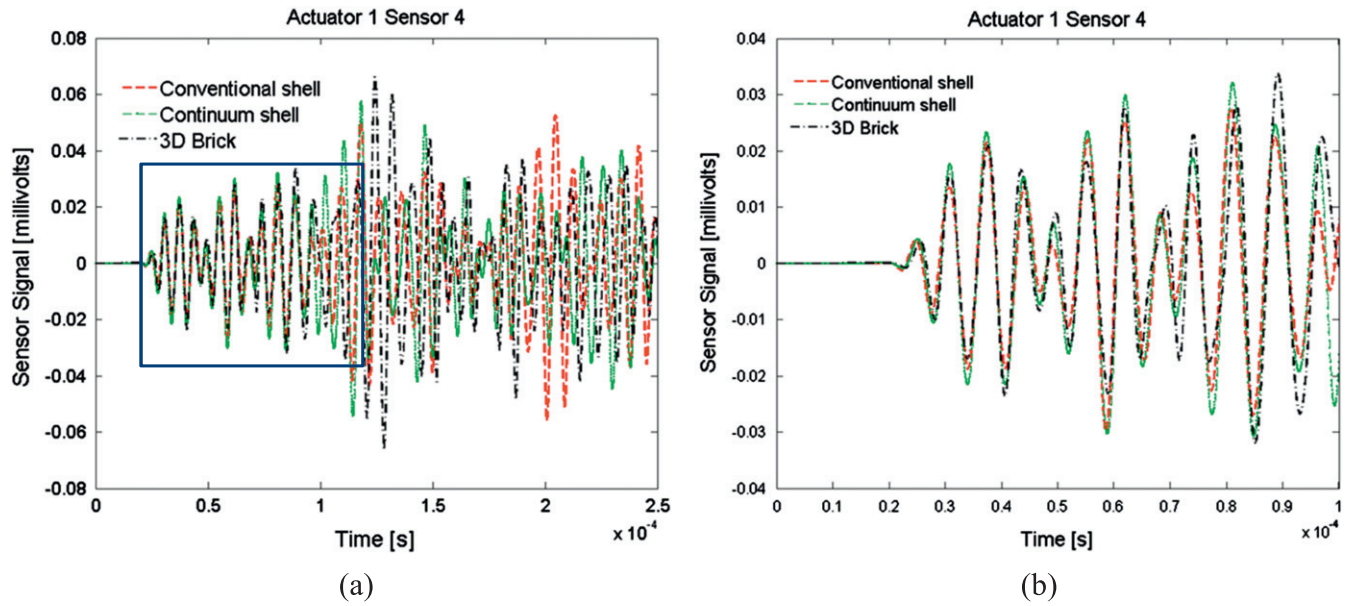
Figure 10. Comparison of different modelling techniques for composite laminates. (a) Full signal. (b) Detailed signal, first modes.
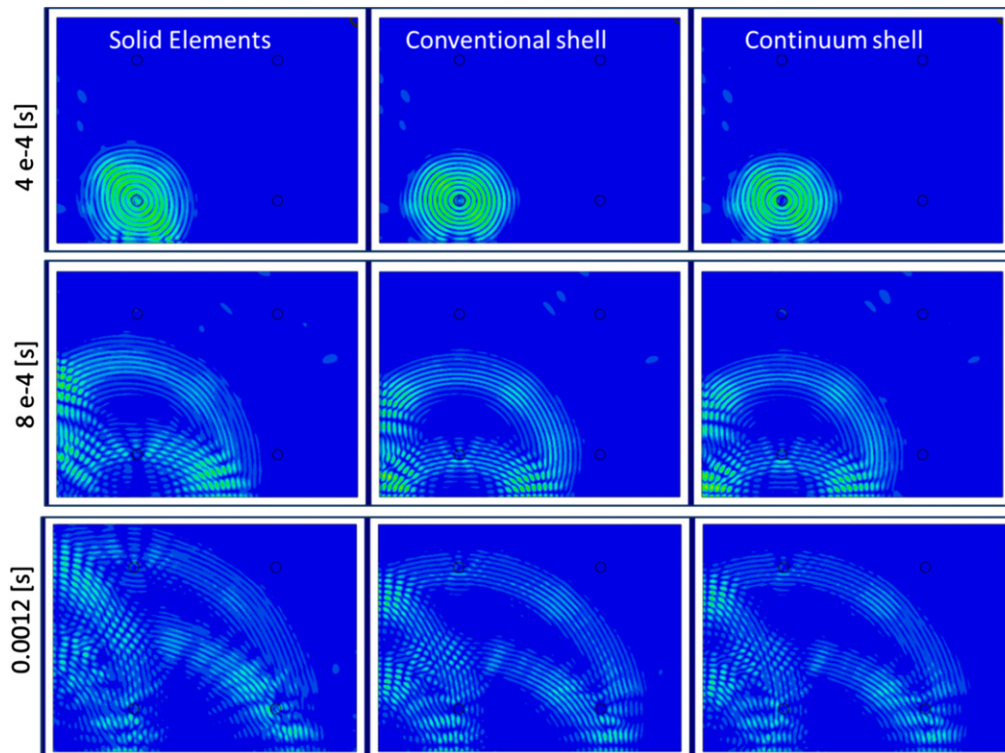

Figure 11. Wave propagation in the plate modelled with solid, conventional shell and continuum shell.

reported in the previous section. The phase and wave shape of the first modes coincide well between the experiment and numerical model. As the wave progresses further the mismatch becomes more pronounced. There are several mechanisms which could lead to this mismatch between numerical and experimental results. First of all, Lamb waves dissipate with distance, a phenomenon known as attenuation. The level of attenuation can differ between experiments and the numerical model. In the numerical analysis, the adhesive

layer is modelled explicitly as a fully tied connection. However, in previous studies (Sharif Khodaei *et al* 2013) it has been reported that the presence of the adhesive layer and its thickness influences the amplitude of the sensor signals. The absence of the adhesive layer can cause the difference between the two signal amplitudes seen in figure 12(b). Other factors which could contribute to the mismatch between numerical and experimental results are damping factor, numerical modelling of out of plane displacements in
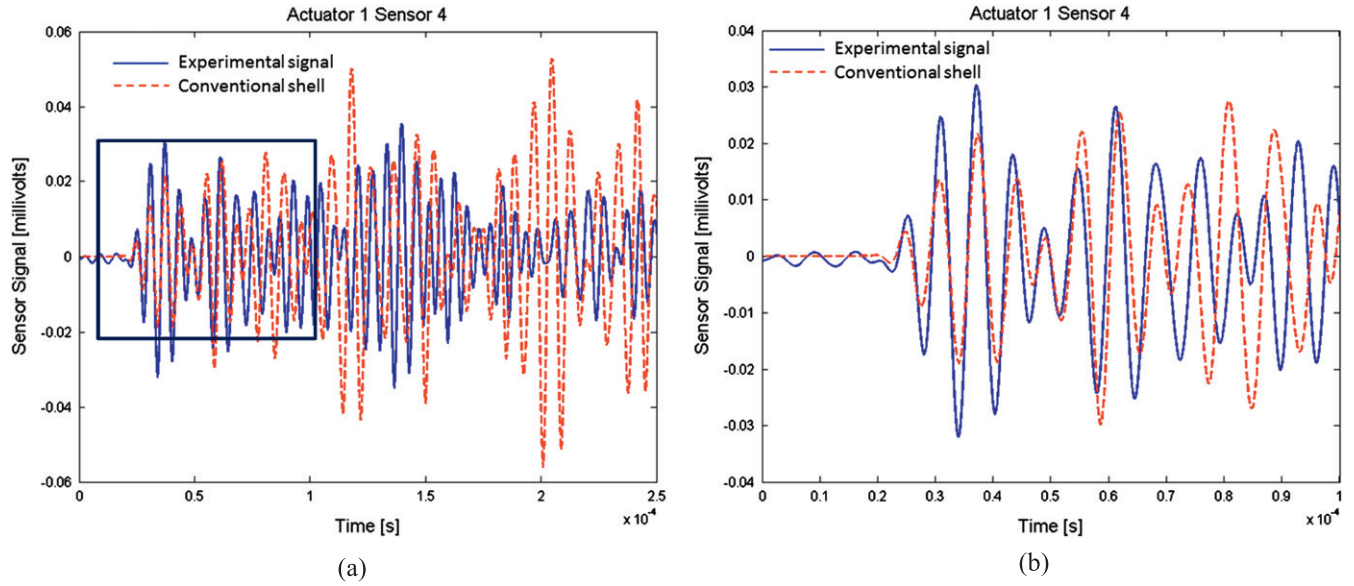
Figure 12. Numerical signal versus experimental signal. (a) Full signal. (b) Detailed signal, first modes.

composite laminas (anti-symmetric mode), geometric toler-ances such as thickness of the plate, position of the transdu-cers, etc. It is well known that for a dynamic problem such as wave propagation in composite laminates it is very difficult to get an exact match between experiments and numerical results. One way to address this would be to investigate the use of spectral elements for this application (Kijanka *et al* 2013). Since the proposed damage detection algorithm is mainly based on the difference between the first arrival modes and the first modes of both numerical and experimental sig-nals coincide well, the signals are considered validated for the purpose of this work.

4. Damage detection algorithms

In this section, different damage detection algorithms based on the delay-and-sum method are tested and evaluated. The two main procedures investigated are the RAPID algorithm proposed by Zhao *et al* (2007) and delay-and-sum imaging algorithm modified by Michaels (2008) which are the starting point of many developed damage detection methodologies (Fu *et al* 2013, Kwon *et al* 2013, Qiu *et al* 2013).

4.1. RAPID

In their study Zhao *et al* (2007) developed a correlation analysis to detect small defects by measuring the difference in guided wave signals between pristine and damage condition. A correlation coefficient is introduced as

$$\rho = \frac{C_{XY}}{\sigma_X \sigma_Y} \qquad (1)$$

where C_{XY} is the covariance of the pristine data set X and each new set Y recorded during the service time, σ_X and σ_Y are the standard deviations of X and Y. The location of the defect is determined by the severity of signal changes of different
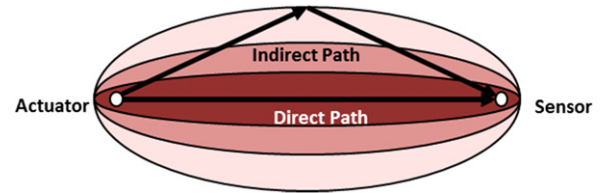

Figure 13. Elliptical distribution function of probability of defect location—RAPID.

sensor pairs as a result of the defect. The location is then expressed as a probability of defect distribution by a linear summation of the correlation coefficients from all actuator-sensor pairs. The spatial distribution of defect probability is assumed to be linearly decreasing elliptical distribution as shown in figure 13. The size of the elliptical distribution function is controlled by a scaling parameter β. Zhao *et al* (2007) have suggested that β is usually selected to be around 1.05. In general, when a defect occurs, the sensor signals will be affected and consequently the defect distribution prob-ability image will have higher probability where the defect is located compared to other points. By applying image pro-cessing techniques the defect location can be estimated.

To check the applicability of both algorithms and compare the results against the published data, the same problem which has been presented in Michaels (2008) is solved here. An aluminium plate of dimensions $610\,\mathrm{mm} \times 610\,\mathrm{mm} \times 4.76\,\mathrm{mm}$ has been instrumented with an array of six PZT transducers as shown in figure 14(a). Damage has been introduced in the form of a 6 mm diameter hole. The actuation signal was a three-cycle sine-burst signal with the central frequency of 250 kHz. The sensor signals for this problem were obtained numerically (using the validated model presented in section 3). All actuator-sensor paths were used in damage detection.

Figure 14 shows the results of defect location using RAPID. It can be observed that the choice of correlation
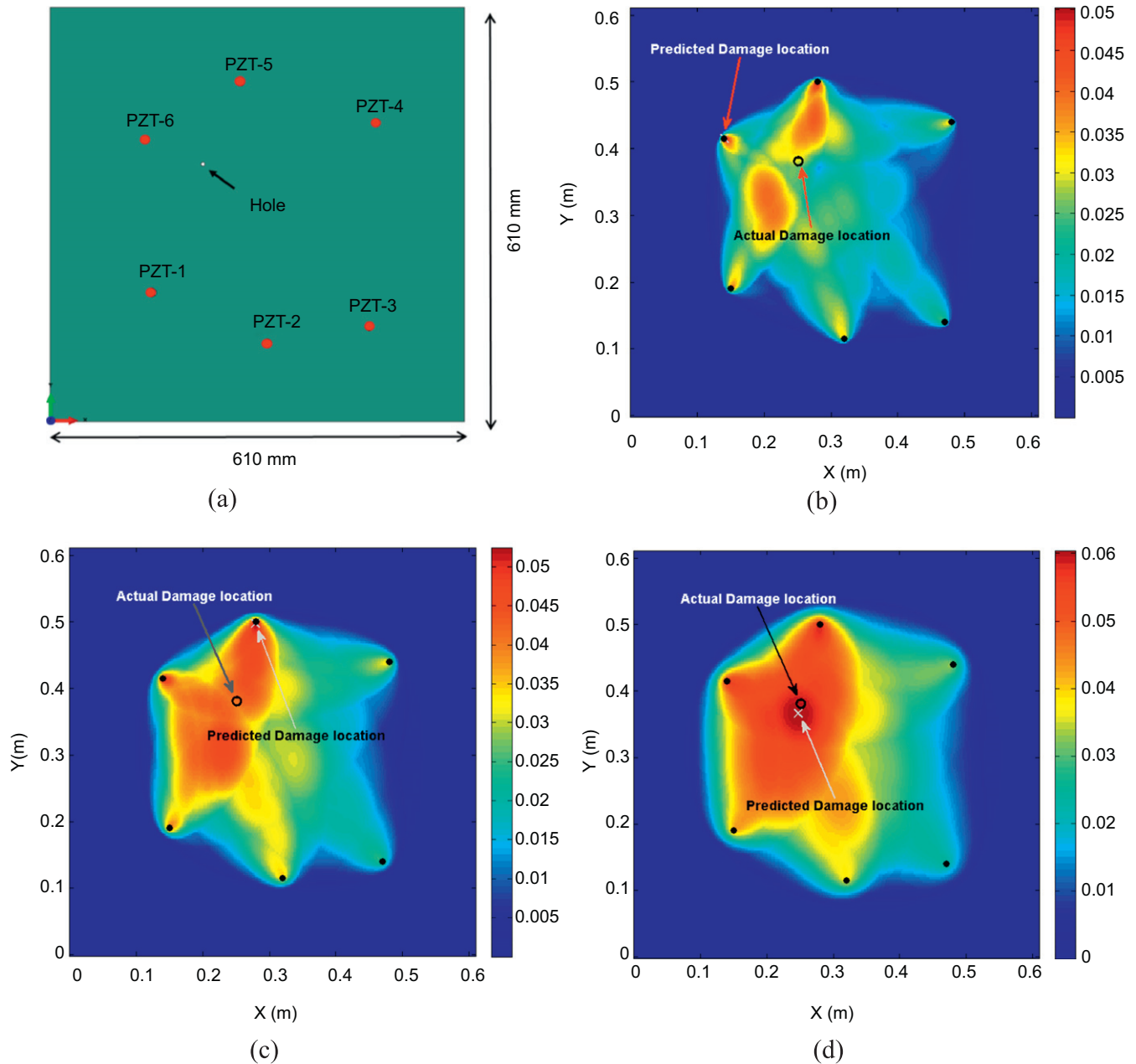
Figure 14. Damage detection using RAPID algorithm (b)–(d) using different scaling parameters β. (a) Plate geometry. (b) $\beta = 1.05$. (c) $\beta = 1.1$. (d) $\beta = 1.2$.

coefficient β plays an important role in detecting and localizing damage. For $\beta = 1.05$ and $\beta = 1.1$ the damage was not detected correctly. One disadvantage of the RAPID is that it gives high defect probability at the location of transducers. This can lead to false positives (see figures 14(b), (c)). For $\beta = 1.2$ the damage was detected close to the actual damage (figure 14(d)), however the extent of damage shown is too great. Moreover, to detect and localize damage a high number of transducer paths needs to be used to cover the whole plate, even for a small size plate.

The composite plate described in section 2.2 was impacted with 5.83 J (2.2 m s^{-1} velocity, 2.41 kg mass) 50 mm off centre in the x direction at the point (200,112.5) mm, to cause BVID in the plate (C-scan image of

the plate confirmed presence of damage). Using four sensors it was not possible to detect the damage using RAPID, see figure 15.

The C-scan of the plate after impact showed that the damage is approximately centred at (202.5, 112.5) mm.

The second plate, the stiffened plate presented in section 2.2, was impacted as well. The impact energy was the same as the unstiffened plate to cause BVID. The impact position was under the stiffener in the centre of the plate and sensor readings were collected before and after the impact. Using the RAPID algorithm the damage could not be located using only four sensors. It can be seen in figure 16 that the value of damage index in the middle of the plate is shown to be slightly higher than the min value. Nevertheless, more
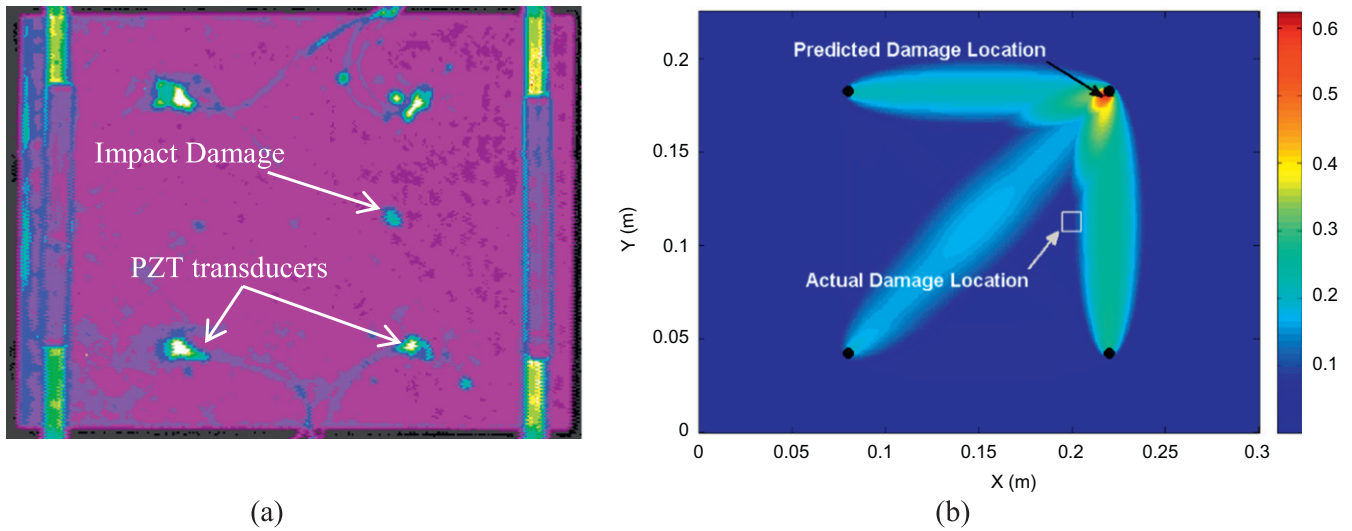
Figure 15. Damage detection in composite plate—experimental results. (a) C-scan image of impacted plate. (b) Damage detection using RAPID.
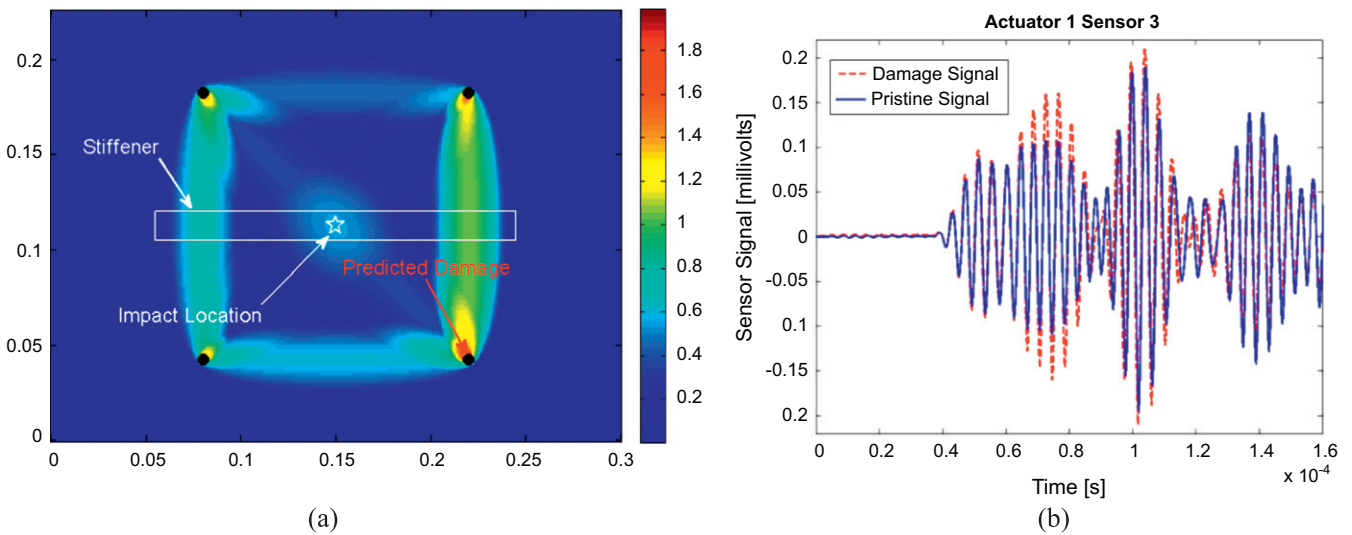

Figure 16. Composite stiffened plate. (a) Damage detection using RAPID. (b) Pristine vs damage signal—250 kHz.

transducer paths are necessary to detect the damage correctly. This is one of the main drawbacks of the RAPID algorithm. In addition, the high probabilities at the locations where transducers are attached adds to the error.

In the case of impact damage in composites, where the damage type is delamination and fibre/matrix breakage there are no distinct reflections from the damage, but rather changes in amplitude and waveform (figure 16(b)) which makes the detection more complex in comparison to through thickness holes and cracks as presented by Zhao *et al* (2007).

4.2. Delay-and-sum algorithm

The delay-and-sum algorithm is based on the residual signal obtained by subtracting the signals, recorded at the current state of interest, from a baseline signals corresponding to the

pristine state. The residual signals from all the actuator-sensor paths are then shifted according to an appropriate time shifting rule and then summed to yield an average signal (Michaels and Michaels 2007).

In the delay-and-sum algorithm the ToAs of the propagated waves need to be calculated accurately given a specific path; therefore the accurate knowledge of group velocity is of high importance. Lamb waves are dispersive and both the phase and group velocities are functions of frequency and plate thickness. It is assumed that a single mode is dominant and is used for damage detection, which for our experiments is the first symmetric mode S_0.

Consider the ith transducer pair where the actuator is located at $\left(x_i^a, y_i^a\right)$ and the sensor located at $\left(x_i^s, y_i^s\right)$. If there is a defect located at (x_n, y_n), it will cause the wave to scatter and
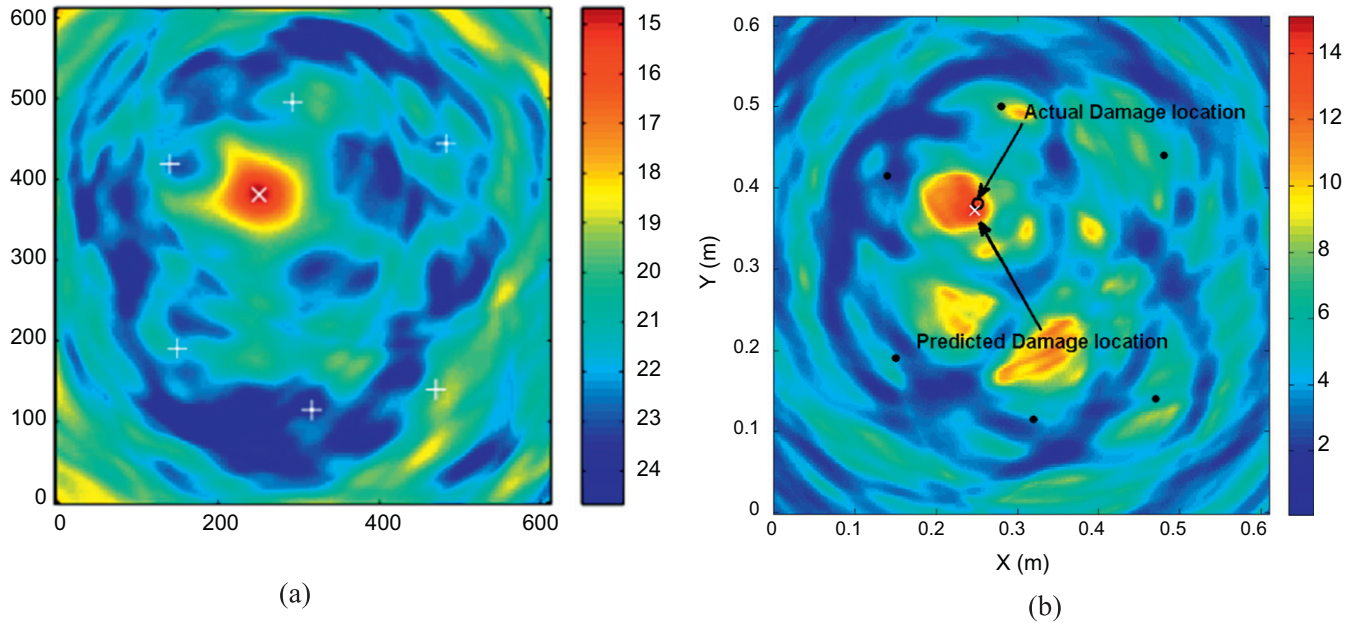
(a)

(b)

Figure 17. Damage detection in an aluminium plate using the delay-and-sum algorithm. (a) Published results by Michaels (2008). (b) Results obtained using numerical model and modified algorithm.

the time that it will take for the wave to travel from actuator to the defect and back to the sensors is

$$t_i^{xy} = t_{off} + \frac{|r_i^a| + |r_i^s|}{c_g} \tag{2}$$

where c_g is the group velocity, and $|r_i^a| = \sqrt{(x_i^a - x_n)^2 + (y_i^a - y_n)^2}$ is the distance from actuator to the imaging point (x_n, y_n). The structure is divided into pixels considering each pixel as an image point (x_n, y_n) and for each location the residual is calculated at the travelled time t_i^{xy} (time which took for the wave to travel from the actuator to the pixel and back to the sensor). The sums of residual signals are then input to an imaging algorithm to fuse multiple images generated by each transducer pair resulting in damage detection and characterization. The residual signal is measured as the magnitude of the complex analytical signal:

$$r_{ij}(t) = \sqrt{u_{ij}(t)^2 + v_{ij}(t)^2} \tag{3}$$

Following the delay-and-sum algorithm proposed by Michaels (2008) each differenced signal is delayed, squared and averaged at each spatial location:

$$E(x, y) = \frac{1}{N} \sum_{i=1}^{N-1} \sum_{j=i+1}^{N} r_{ij}\left(t_{ij}(x, y)\right) \tag{4}$$

In this section, the same problems presented in section 4.1 are solved using the delay-and-sum algorithm to compare with the published results and the RAPID algorithm. Figure 17 shows good agreement between the published results which were obtained using experimental signals and our results achieved by means of numerical signals.

However, the above example is an aluminium plate (isotropic) and the detectable damage is a through thickness hole which is much easier to detect since the edges of the opening scatter and reflect the waves significantly. The question still remains whether the algorithm is applicable to more complicated structures and different types of damage such as delamination and softening which are barely visible. Therefore the second step was to test it on our composite plates introduced in section 2.2.

By actuating all four transducers in turn, 12 transducer paths are recorded. However, due to reciprocity, the experimental signals corresponding to six paths are input to the delay-and-sum algorithm to detect damage. Figure 18(a) shows the result of the damage detection algorithm. The damage was detected at (166.5, 122.6) mm in comparison to actual damage location at (200, 112.5) mm.

The stiffened plate was also evaluated using the delay-and-sum algorithm to find the damage and the result is presented in figure 18(b). The results of the two examples show that for the case where the plate was damaged in the centre, damage was detected at its exact location, even though the extent of damage was more than the actual size of damage. However, when the damage was off-centre the accuracy was decreased significantly. One reason for this is that less transducer paths are directly passing through damage since the direct paths have the most significant change on the signal. Another reason is that off-centre damage eradicates the symmetry of the problem. Therefore, to increase the accuracy of damage localization, more sensor-actuator paths are necessary. Subsequently, modifications to the delay-and-sum algorithm can improve the damage localization and characterization.
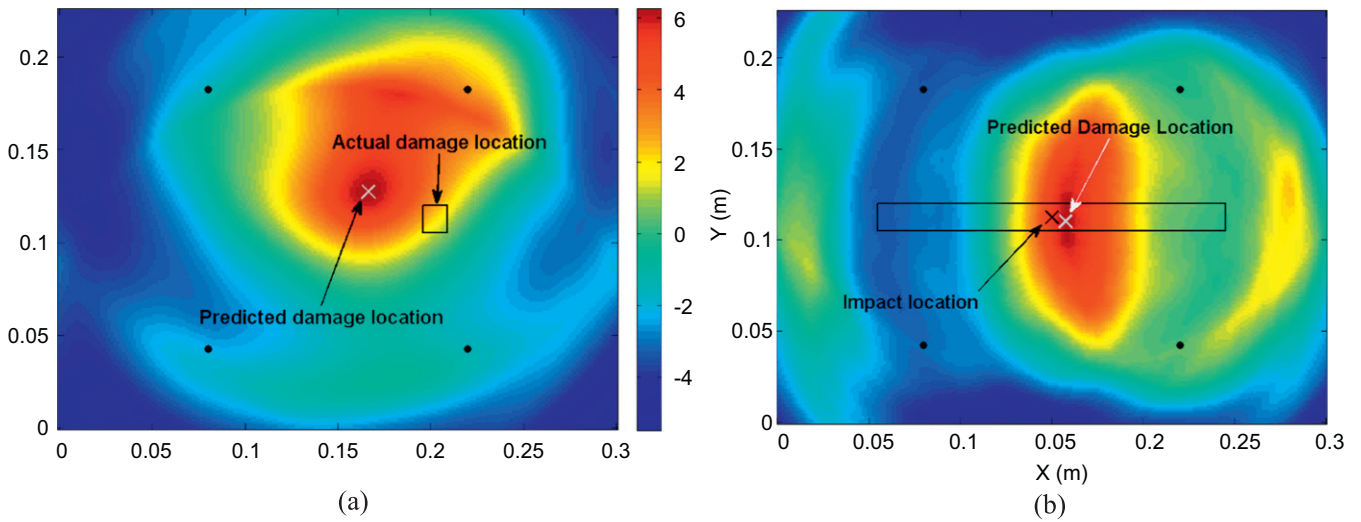
Figure 18. Impact damage detection using the delay-and-sum algorithm. (a) Composite plate. (b) Composite stiffened plate.
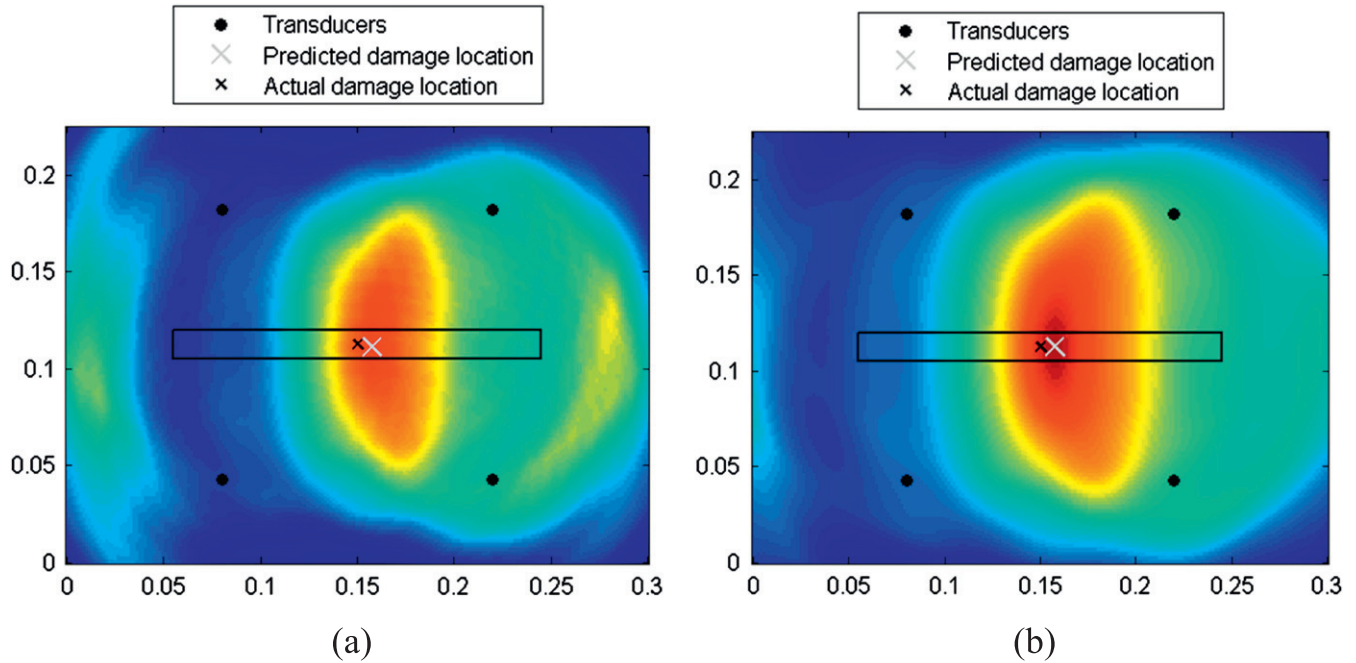

Figure 19. Damage detection results obtained with different signal processing techniques. (a) Results obtained with Hanning-windowed filter. (b) Results obtained by Butterworth filter.

5. Proposed windowed energy arrival method (WEAM)

To improve the results of the delay-and-sum algorithm a WEAM with several modifications is proposed in this section:

5.1. Pre-processing of acquired signals

Michaels *et al* (2008) filtered the signals using time domain convolution with a Hanning-windowed toneburst. However, it was noticed that by applying wavelet transform or band-pass filter, a better denoising of the signal is achieved. This is apparent from figure 19 which shows the results of the damage detection of the stiffened composite panel, obtained

with filtering the experimental signals. The results are plotted in the same scale to be comparable. Figure 19(b) has better damage localization and contains less noise. Both wavelet and butterworth filters resulted in the same denoised signals. Therefore, the authors have proposed applying butterworth band-pass filter to minimize the effect of cross-talk and noise in measuring the ToA of the first arrival mode and the damage reflected wave t_i^{xy}. Moreover, each signal has been normalized with the peak of the first arrival packet.

5.2. ToA and group velocity

The accuracy of the proposed algorithm is highly dependent on the accuracy of the group velocity of the first arrival wave
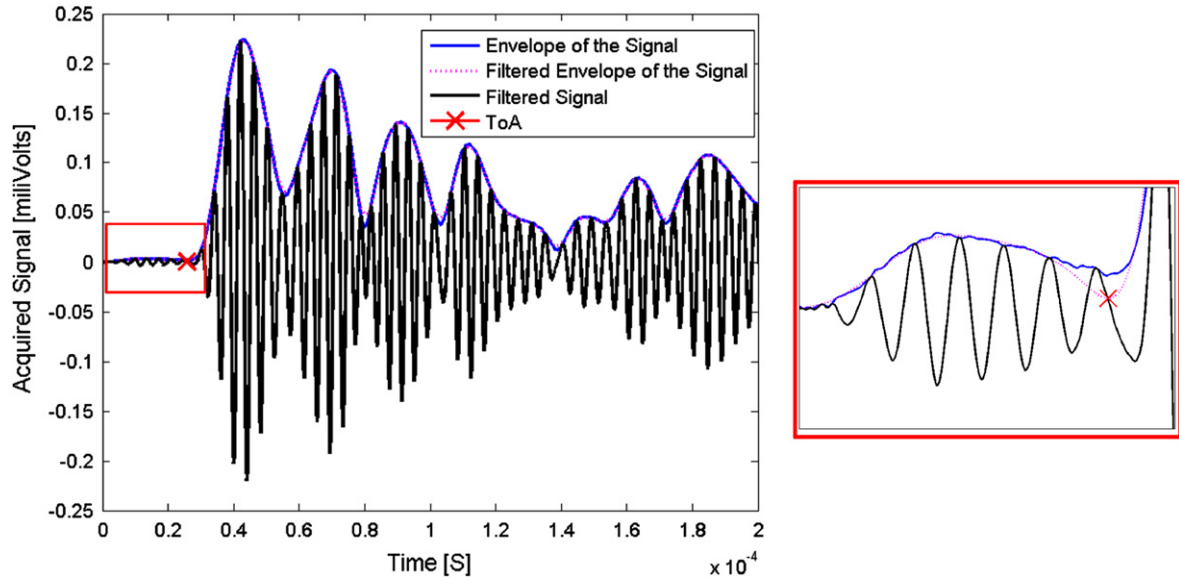
Figure 20. ToA of the wave measured from the envelope of the signal.

packet. Michaels *et al* (2008) measured the group velocity of the waves by plotting a waterfall plot of the acquired signals versus the propagation distances. However, the presence of cross-talk can interfere with measuring the ToA of the wave packet. Therefore, by simply defining a threshold for the arrival signal, the ToA cannot be measured correctly. The authors have proposed measuring the ToA from the envelop of the travelled wave rather than the actual wave. Moreover, the signal envelop has been filtered to remove the noise which can change the results. Figure 20 shows the ToA for the direct path 1–4 with a red cross. By dividing the distance of the travelled wave by ToA the group velocity for the path is measured. The algorithm automatically measures the ToA of each path and plots it against the propagation distance. The slope of the fitted curve is the group velocity of the first arrival mode. The measured group velocity without filtering the envelope is $5102 \, \mathrm{m \, s^{-1}}$ compared to $5488 \, \mathrm{m \, s^{-1}}$ which is the result of filtering the envelop signal. The results obtained with $5488 \, \mathrm{m \, s^{-1}}$ is improved, specifically in terms of magnitude of DI. Figure 21 presents both results plotted in the same scale. The value of DI is of high importance for sizing and characterizing damage (figure 22).

5.3. WEAM

Another modification of the proposed algorithm is in obtaining the Damage Index (DI) used in the imaging algorithm for each pixel (x, y). DI is defined as the value of the envelope of the differenced signal r_{ij} at a given time t_{ij} for all transducer paths ij (actuator i, sensor j):

$$DI(x, y) = \frac{1}{N} \sum_{i=1}^{N} \sum_{j=1}^{N} r_{ij}\left(t_{ij}(x, y)\right) . w_{ij}(\sigma, v) \qquad (5)$$

where N is the number of transducer pairs, and $w_{ij}(\sigma, v)$ is a window function with log-normal distribution. The damage detection is based on the damage reflected wave from the first mode, i.e. the first peak of the residual envelope signal referring to the difference in energy transferred in both states. Therefore,

to focus the DI measurement on the first damage reflection and avoid the secondary reflections from boundaries and/or superposition of higher modes, the envelop detected residual signal is weighted by a log-normal distribution having the mean v centred at ToA of the damage reflected wave. Furthermore, a threshold for the DI measure is introduced in the fusion algorithm to plot only positive values.

Most of the published algorithms based on delay-and-sum, including the work by Michaels and Zhao *et al* assume reciprocity of the solution and therefore only use $N = N(N-1)/2$ paths in the above equation. This means that the recorded signal in sensor 2 from actuator 1 should be equal to signal in sensor 1 from actuator 2. This is true only when damage is not present in the structure since the damage will disturb the symmetry of the problem, or if we can ensure that the damage is symmetric which is not expected as a result of an impact on a composite plate. This effect is more pronounced for the paths directly passing through damage. If we examine path 1–2 and 2–1 of the stiffened panel impacted in the centre, which are far from damage, no significant change can be noticed between the two signals (figure 23(a)). In contrast, when the signal passes through the damaged area the reciprocity is lost and both paths should be considered in calculating DI (equation (5)).

The results of the damage detection for both stiffened and flat composite panels, applying the improved algorithm, are shown in figure 24(b) and figure 25(b). Comparing the results with figures 18(a) and (b) apparent improvements can be seen in the results, mainly in the extent of the damage. It is evident from the results that using all paths for measuring the DI improves the results. By applying a threshold to the algorithm, the damage could potentially be sized and its severity characterized. This will be investigated in future works.

In the case of the composite panel with off-centre impact, damage has been detected (DI values above zero) but the location of damage is not very accurate. It is still good results considering that BVID was detected by using only four transducers. The results can be improved by adding more
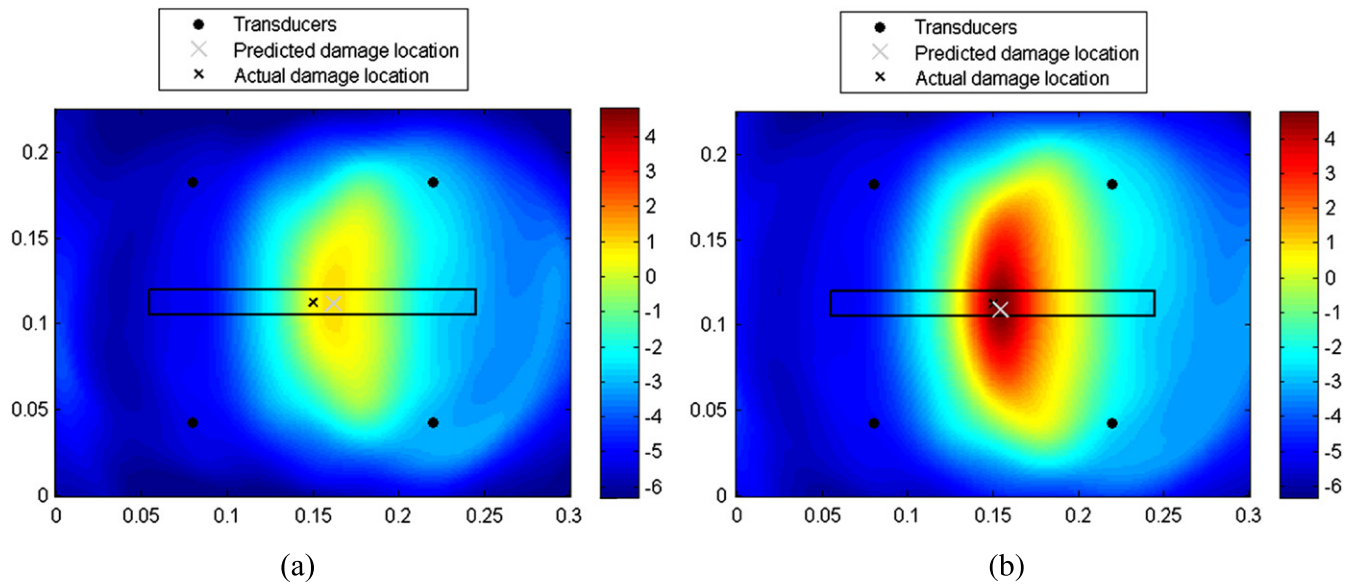
(a)   (b)

Figure 21. Influence of group velocity on damage detection. (a) Group velocity 5102 m s^{-1}. (b) Group velocity 5488 m s^{-1}.

(a)   (b)
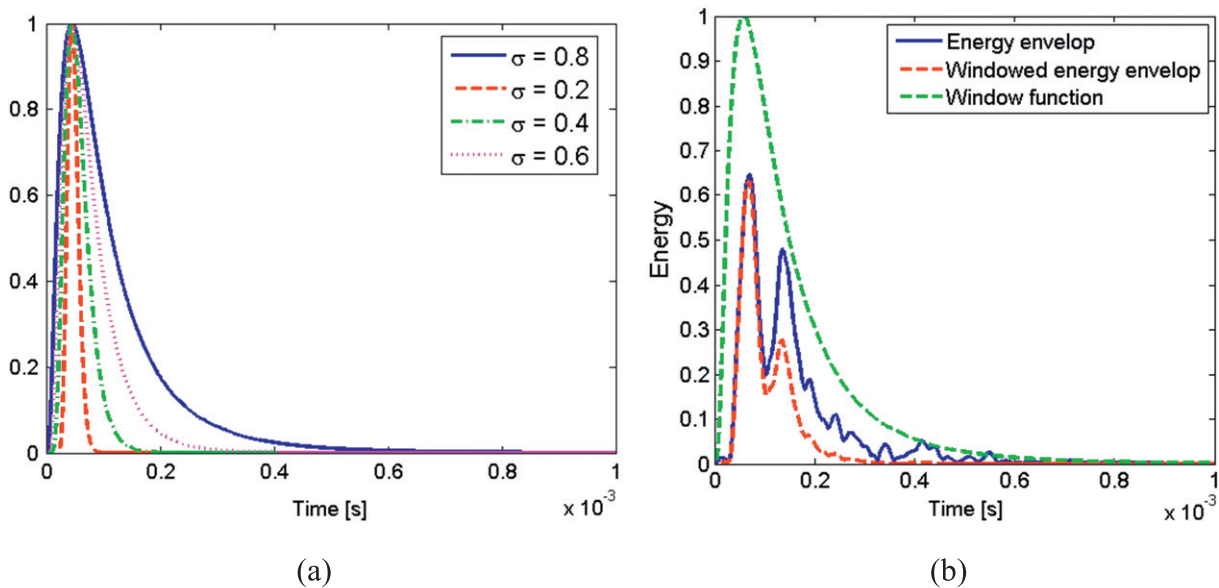
Figure 22. An example of the weighted signal envelope path 1–4. (a) Weighting function. (b) Influence of the weighting function.

transducer paths. The proposed methodology can be used as first level of damage detection with the aim to detect and localize damage to a specific area in the structure with the minimum number of transducers. Second level detection can then include acquiring more paths or using methods which is more appropriate for local detection. This will be investigated in future works.

6. Results and discussion

In the previous section, it was shown that the proposed delay-and-sum algorithm is capable of detecting and locating impact damage in composite panels with adequate accuracy, given

the low number of transducers. In this section, different features of the proposed algorithm are investigated.

6.1. Damage detection using numerical signals

To compare the validity of the proposed numerical model for damage detection, the composite panel tested in section 2.2 has been modelled and analysed. Damage was introduces as 50% softening (degradation of the elastic material properties) in layers four, five and six of the composite laminate in an area of 100 mm^2, corresponding to the damage area of the impacted plate. The sensor signals were recorded and used in the modified delay-and-sum algorithm to detect damage. The results of the damage detection using two different spatial variations for DI are presented in figure 26.
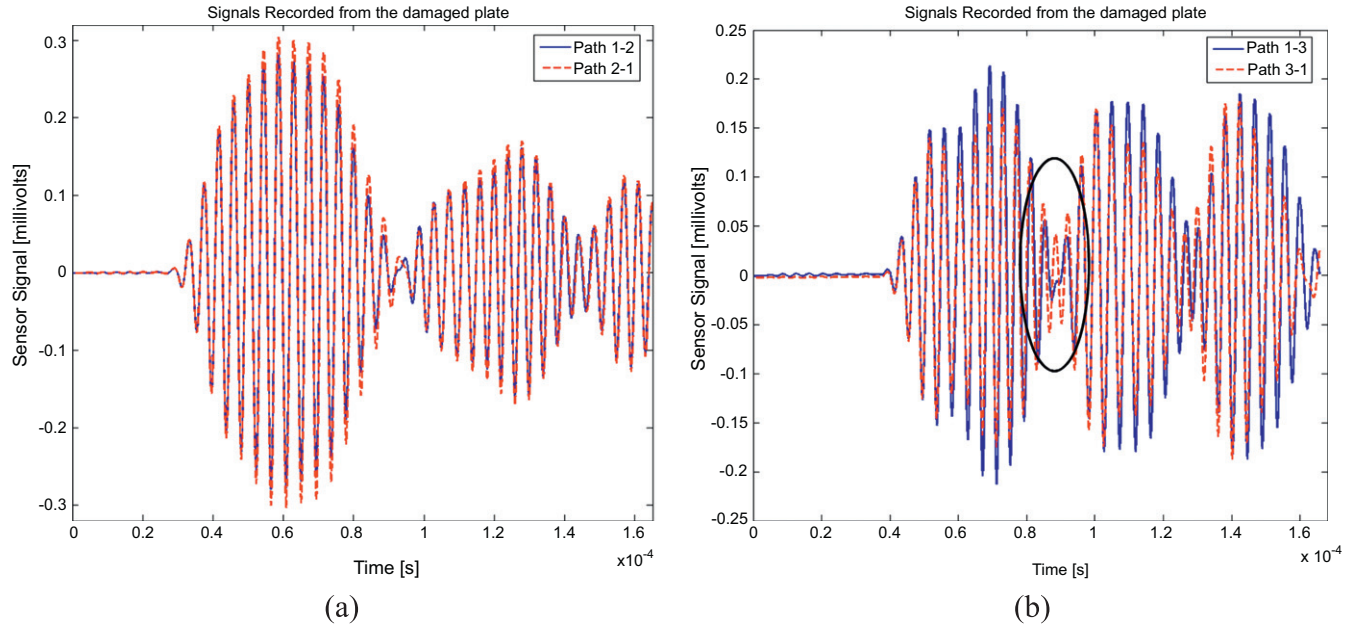
Figure 23. Reciprocity of path *ij* and *ji*. (a) Paths 1-2 and 2-1 far from damage. (b) Paths 1-3 and 3-1 passing through damage.
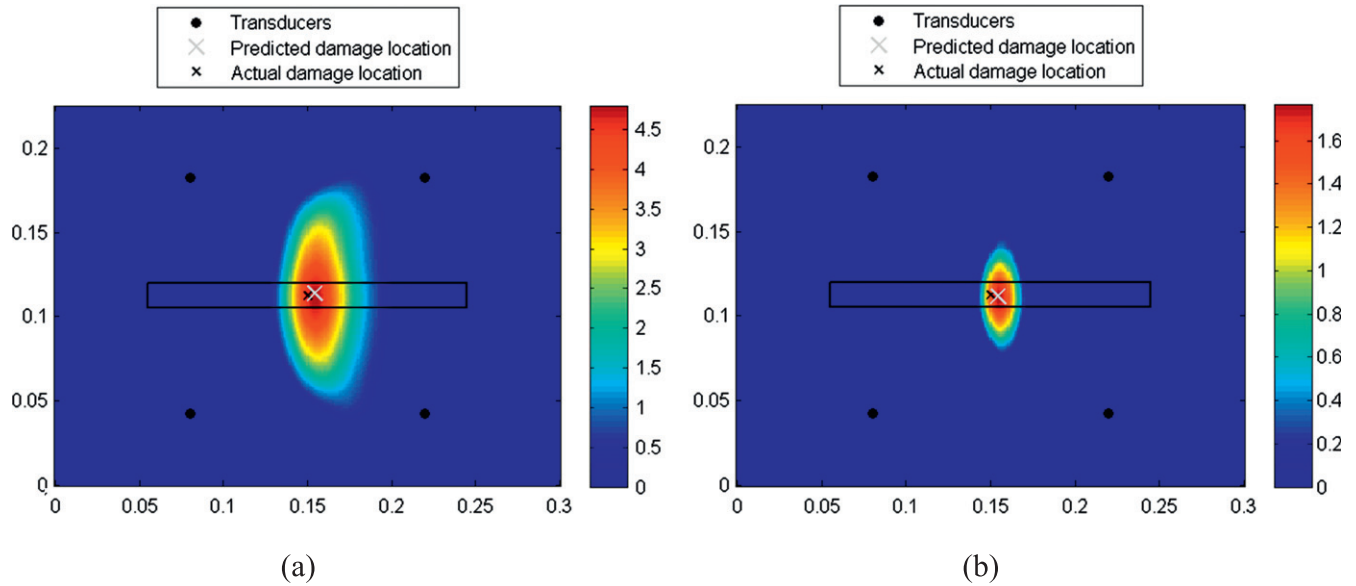

Figure 24. Improved delay-and-sum algorithm applied to the stiffened composite panel. (a) DI measured from reciprocity of paths. (b) DI measured from all possible paths.

The results of the damage detection using numerical signals shows a better prediction of the damage location and its extent (figure 26) compared to the experimental case (figure 25(b)). There are various reasons why numerical signals result in better prediction of damage, some of which can be listed as:

- Absence of noise (environmental and hardware noise) and cross-talk in numerical data
- Tolerance of sensor positioning and dimensions of the plate

- The defined boundaries of the damage area which can reflect a stronger wave
- No manufacturing fault
- No environmental effects such as temperature and moisture
- Symmetric damage in all three laminates

The factors listed above indicate the importance of de-noising and filtering of the signals, as well as repeatability of the experiments under different environmental conditions.
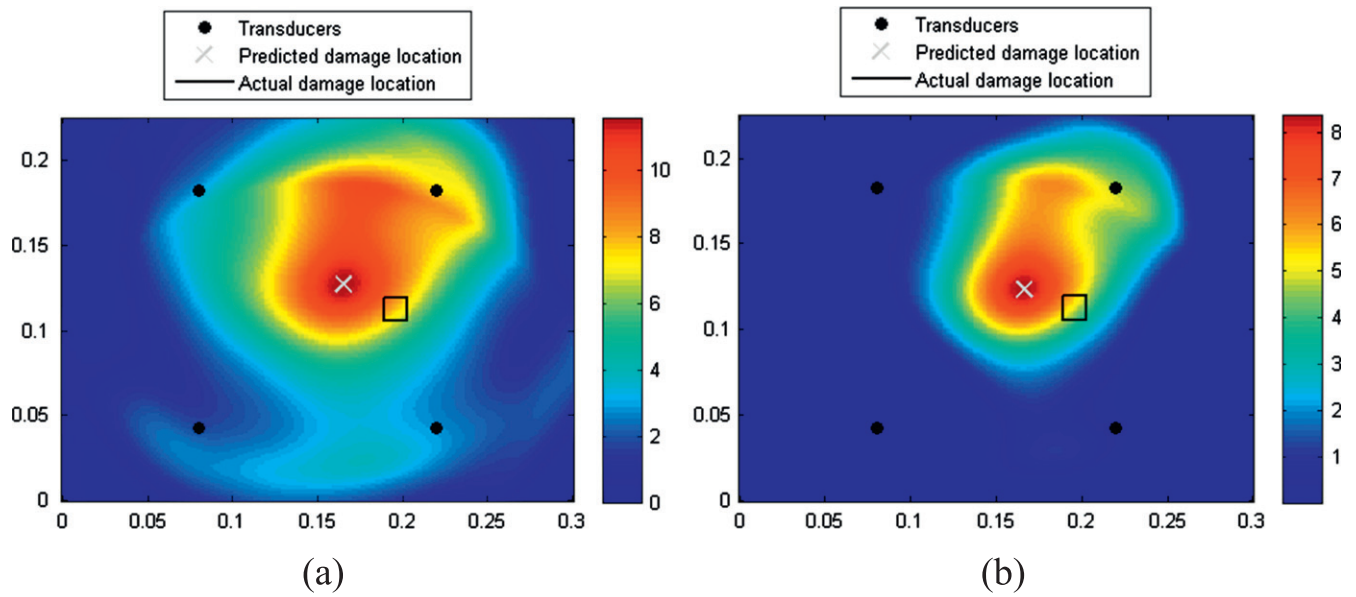
Figure 25. Improved delay-and-sum algorithm applied to the flat composite panel. (a) DI measured from reciprocity of paths. (b) DI measured from all possible paths.
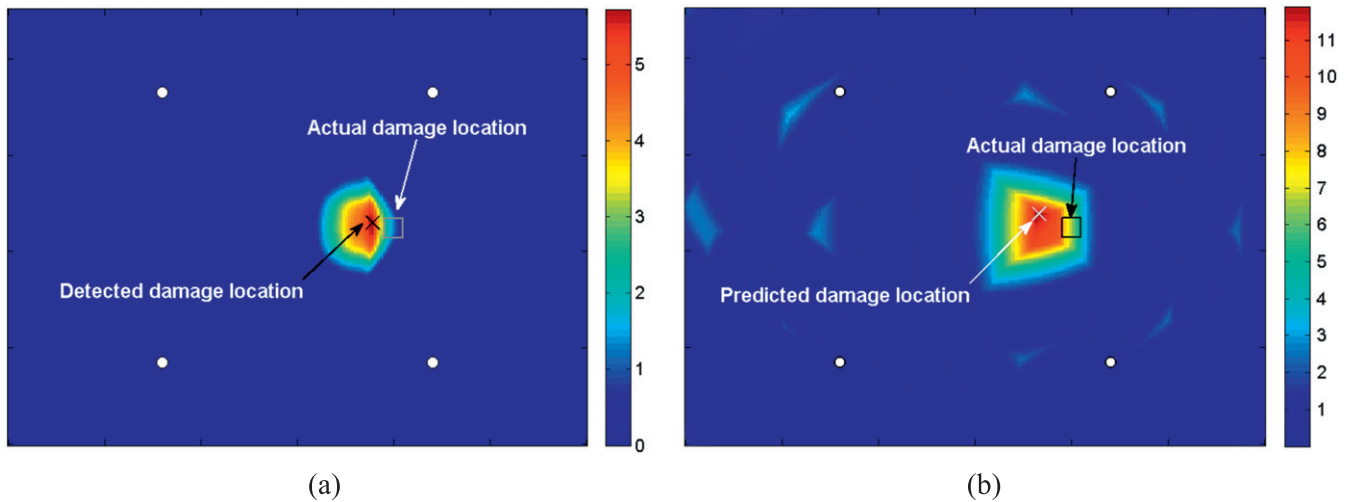

Figure 26. Damage detection based on numerical sensor signals, various fusion algorithms. (a) Sum of the distribution of DI. (b) Max DI for each pixel.

7. Conclusion

The delay-and-sum algorithm has been assessed for detecting BVID in isotropic and composite plates, for both simple and stiffened panels. In particular, two main delay-and-sum algorithms which are the basis of various proposed methodologies, are evaluated: the RAPID algorithm proposed by Zhao *et al* (2007) and the delay-and-sum imaging method applied to the residual signals published by Michaels (2008). The published methodologies have been validated for aluminium plates with cracks and corrosion only. Therefore the applicability of the proposed methods was tested for composite panels with BVID. The RAPID algorithm showed to be very sensitive to the choice of the correlation factor β. Although it was able to detect damage (a hole) in an aluminium plate, it failed to detect impact damage (delamination,

damage, etc) in a composite panel. The method failed detecting damage in both stiffened and unstiffened composite panels using only four transducers. One of the main drawbacks of the method is flagging up damage at the locations of attached transducers. The delay-and-sum algorithm was evaluated for an aluminium plate as well as the composite panels. In both cases it has shown to be successful in detecting the damage. However, localizing and characterizing the damage in the composite plates were not accurate.

An improved algorithm based on windowed energy arrival has been proposed. Modifications were made to the algorithm in terms of signal processing, calculating the expected arrival time and spatial variation of DI. The proposed algorithm detected and localized damage in composite panels with and without a stiffener successfully, using only four transducers. The localization and sizing of the damage

has been improved using the WEAM. The improvement of the damage detection algorithm is more pronounced for the case where damage was in the centre. This can be improved by adding more transducer paths for the off-centre damage. The influence of two types of fusion algorithms have been studied and reported.

A numerical model based on commercial FE software, in combination with analytical sensor models, was investigated and validated against the experimental results for the wave propagation in isotropic and composite panels. Damage was introduced in the model in a rectangular area of $100\,\mathrm{mm}^2$. In addition, the numerical signals were input to the proposed damage detection algorithm to compare the results with the experiments. The numerical results showed better detection capabilities in comparison to the experimental results. This is related to many factors such as absence of noise, cross-talk, geometric tolerance, environmental effects, etc. However the authors believe and important factor is unsymmetrical nature of impact damage. Impact damage in composites have a complex nature which affects the signal reflections and refractions. Therefore an important conclusion can be made that by testing any proposed methodologies on structures where an artificial damage is introduced (for example additional mass) it is not sufficient to indicate that the method will be successful in case of a real impact damage.

Future work will contain further application and validation of the proposed algorithm for structures of larger scale, complex geometries and layup. In addition the PoD and PoFA values need to be addressed.

Appendix

References

Alleyne D and Cawley P 1991 A two-dimensional Fourier transform method for the measurement of propagating multimode signals *J. Acoust. Soc. Am.* **89** 1159

Bartoli I *et al* 2006 Modeling wave propagation in damped waveguides of arbitrary cross-section *J. Sound Vib.* **295** 685–707

Ben B *et al* 2012 Damage identification in composite materials using ultrasonic based Lamb wave method *Measurement* **46** 904–12

Benedetti I *et al* 2010 A fast BEM for the analysis of damaged structures with bonded piezoelectric sensors *Comput. Methods Appl. Mech. Eng.* **199** 490–501

Cobb A C *et al* 2009 Ultrasonic structural health monitoring: a probability of detection case study *Review of Quantitative Nondestructive Evaluation* vol 28 pp 1800–7

Delsanto P P and Scalerandi M 1998 A spring model for the simulation of the propagation of ultrasonic pulses through imperfect contact interfaces *J. Acoust. Soc. Am.* **104** 2584

Diamanti K *et al* 2005 Lamb waves for the non-destructive inspection of monolithic and sandwich composite beams *Composites* A **36** 189–95

Fedelinski P *et al* 1997 The time-domain DBEM for rapidly growing cracks *Int. J. Numer. Methods Eng.* **40** 1555–72

Fromme P *et al* 2006 On the development and testing of a guided ultrasonic wave array for structural integrity monitoring *IEEE Trans. Ultrason. Ferroelectr. Freq. Control* **53** 777–85

Fu S C *et al* 2013 A method of dispersion compensation based on warped frequency transform. *Adv. Mater. Res.* **718** 2062–7

Ghajari M *et al* 2013 Identification of impact force for smart composite stiffened panels *Smart Mater. Struct.* **22** 085014

JSSG 2006 Joint service specification guide *Aircraft Structures*

Kessler S S *et al* 2011 A structural health monitoring software tool for optimization, diagnostics and prognostics *DTIC Document*

Kessler S S *et al* 2002 Damage detection in composite materials using Lamb wave methods *Smart Mater. Struct.* **11** 269

Kijanka P *et al* 2013 GPU-based local interaction simulation approach for simplified temperature effect modelling in Lamb wave propagation used for damage detection *Smart Mater. Struct.* **22** 035014

Table A1. T700/M21 material properties.

E_1 (GPa)	E_2	E_3	ν_{12}	ν_{13}	ν_{23}	G_{12} (GPa)	G_{13}	G_{23}	$\rho(\,\mathrm{kg\,m^{-3}})$
148	7.8	7.8	0.35	0.35	0.35	3.8	3.8	2.9	1072

Table A2. NEC51 material properties: Elastic rigidity matrix E—C^E (N m^{-2}).

1.292E + 11	8.640E + 10	8.306E + 10	0.000E + 00	0.000E + 00	0.000E + 00	xx
8.640E + 10	1.292E + 11	8.306E + 10	0.000E + 00	0.000E + 00	0.000E + 00	yy
8.306E + 10	8.306E + 10	1.169E + 11	0.000E + 00	0.000E + 00	0.000E + 00	zz
0.000E + 00	0.000E + 00	0.000E + 00	2.883E + 10	0.000E + 00	0.000E + 00	xy
0.000E + 00	0.000E + 00	0.000E + 00	0.000E + 00	2.883E + 10	0.000E + 00	xz
0.000E + 00	0.000E + 00	0.000E + 00	0.000E + 00	0.000E + 00	2.141E + 10	yz

Table A3. Electrical permittivity.

ε_{11}^S	1.106 773 750 00E − 08
ε_{22}^S	1.106 773 750 00E − 08
ε_{33}^S	6.640 642 500 00E − 09

Table A4. Voltage coefficient matrix—E (C m^{-2}).

0	0	0	0	15.149 277	0
0	0	0	15.149 277	0	0
−3.838 136	−3.838 136	16.519 761	0	0	0

Dielectric constant: $\varepsilon_0 = 8.85419\mathrm{E}{-}12\,\mathrm{F\,m^{-1}}$
Density $\rho = 7.80\,\mathrm{kg\,d\,m^{-3}}$

19

Koduru J P and Rose J L 2013 Transducer arrays for omnidirectional guided wave mode control in plate like structures *Smart Mater. Struct.* **22** 015010

Kudela P *et al* 2008 Damage detection in composite plates with embedded PZT transducers *Mech. Syst. Signal Process.* **22** 1327–35

Kudela P *et al* 2007 Modelling of wave propagation in composite plates using the time domain spectral element method *J. Sound Vib.* **302** 728–45

Kwon H-S *et al* 2013 Beam pattern improvement by compensating array nonuniformities in a guided wave phased array *Smart Mater. Struct.* **22** 085002

Lee B and Staszewski W 2003 Modelling of Lamb waves for damage detection in metallic structures: II. Wave interactions with damage *Smart Mater. Struct.* **12** 815

Lindgren E A *et al* 2011 Demonstration study for reliability assessment of SHM systems incorporating model-assisted probability of detection approach *DTIC Document*

Ma J *et al* 2012 Influence of secondary converse piezoelectric effect on deflection of fully covered PZT actuators *Sensors Actuators* A **175** 132–8

Mallardo V *et al* 2012 Optimal sensor positioning for impact localization in smart composite panels *J. Intell. Mater. Syst. Struct.* **24** 559–73

Michaels J 2008 Detection, localization and characterization of damage in plates with an in situ array of spatially distributed ultrasonic sensors *Smart Mater. Struct.* **17** 035035

Michaels J E and Michaels T E 2007 Guided wave signal processing and image fusion for in situ damage localization in plates *Wave Motion* **44** 482–92

Mo C *et al* 2012 Finite element analysis of unimorph rectangular piezoelectric diaphragm actuators with experimental verification *Smart Mater. Struct.* **21** 085025

Ostachowicz W *et al* 2009 Damage localisation in plate-like structures based on PZT sensors *Mech. Syst. Signal Process.* **23** 1805–29

Peng H *et al* 2009 Modeling of wave propagation in plate structures using three-dimensional spectral element method for damage detection *J. Sound Vib.* **320** 942–54

Qiu L *et al* 2013 A quantitative multidamage monitoring method for large-scale complex composite *Struct. Health Monitor.* **12** 183–96

Qiu L *et al* 2013 Digital sequences and a time reversal-based impact region imaging and localization method *Sensors* **13** 13356–81

Radzieński M *et al* 2013 Damage localisation in a stiffened plate structure using a propagating wave *Mech. Syst. Signal Process.* **39** 388–95

Rose J L and Nagy P B 2000 Ultrasonic waves in solid media *J. Acoust. Soc. Am.* **107** 1807

Salmanpour M S 2013 Damage detection in composite materials using piezoelectric sensor/actuators *MEng 4th Year Project* Imperial College, London

Scalerandi M *et al* 2008 Nonlinear acoustic time reversal imaging using the scaling subtraction method *J. Phys. D: Appl. Phys.* **41** 215404

Schwankl M *et al* 2013 Electro-mechanical impedance technique for structural health monitoring of composite panels *Key Eng. Mater.* **525** 569–72

Sharif-Khodaei Z *et al* 2012 Determination of impact location on composite stiffened panels *Smart Mater. Struct.* **21** 105026

Sharif Khodaei Z *et al* 2013 Influence of adhesive layer on actuation of Lamb wave signals *Key Eng. Mater.* **525** 617–20

Soejima H *et al* 2012 Investigation of the probability of detection of our SHM system *6th European Workshop on Structural Health Monitoring (Dresden, Germany)*

Sohn H *et al* 2007 Damage detection in composite plates by using an enhanced time reversal method *J. Aerospace Eng.* **20** 141–51

Su Z and Ye L 2009 *Identification of Damage Using Lamb Waves: From Fundamentals to Applications* (Berlin: Springer)

Wang C H *et al* 2004 A synthetic time-reversal imaging method for structural health monitoring *Smart Mater. Struct.* **13** 415

Watkins R and Jha R 2012 A modified time reversal method for Lamb wave based diagnostics of composite structures *Mech. Syst. Signal Process.* **31** 345–54

Wen P and Aliabadi M 2008 An improved meshless collocation method for elastostatic and elastodynamic problems *Commun. Numer. Methods Eng.* **24** 635–51

Yang C *et al* 2006 Some aspects of numerical simulation for Lamb wave propagation in composite laminates *Compos. Struct.* **75** 267–75

Yim H and Sohn Y 2000 Numerical simulation and visualization of elastic waves using mass-spring lattice model *IEEE Trans. Ultrason. Ferroelectr. Freq. Control* **47** 549–58

Zhao X *et al* 2007 Active health monitoring of an aircraft wing with embedded piezoelectric sensor/actuator network: I. Defect detection, localization and growth monitoring *Smart Mater. Struct.* **16** 1208

Zou F *et al* 2014 A boundary element model for structural health monitoring using piezoelectric transducers *Smart Mater. Struct.* **23** 015022